Physica Scripta

INCLUSIVE PUBLISHING TRUSTED SCIENCE

PURPOSE-LED PUBLISHING™

PAPER

Modeling of Finch-Skea hybrid neutron stars with complexity-free characteristics

To cite this article: S Khan *et al* 2025 *Phys. Scr.* **100** 085302

View the article online for updates and enhancements.

You may also like

- Statistical characterization and numerical investigation of extreme events in a reduced Belousov-Zhabotinsky reaction model
Guang Mei, Juan Zhang, Yao Jiang et al.
- A unified framework for constructing two-dimensional bounded discrete systems
Bei Chen, Jiangning Zhang, Han Bao et al.
- Design of maximum noise transfer path between ship cabins using VAONE
Zhongying Xiong and Yueyao Liu

This content was downloaded from IP address 136.159.213.98 on 25/07/2025 at 23:28

Physica Scripta

PAPER

Modeling of Finch-Skea hybrid neutron stars with complexity-free characteristics

RECEIVED
3 April 2025

REVISED
29 May 2025

ACCEPTED FOR PUBLICATION
10 July 2025

PUBLISHED
24 July 2025

S Khan[1,*], **Javlon Rayimbaev**[2,3,4,5,6], **Inomjon Ibragimov**[7], **Sokhibjan Muminov**[8], **Adilbek Dauletov**[9] and **Ahmadjon Abdujabbarov**[10,11]

[1] University of Agriculture Faisalabad, Constituent College, Toba Tek Singh 36050, Pakistan
[2] National University of Uzbekistan, Tashkent 100174, Uzbekistan
[3] Tashkent International University of Education, Imam Bukhoriy 6, 100207, Tashkent, Uzbekistan
[4] University of Tashkent for Applied Sciences, Str. Gavhar 1, Tashkent 100149, Uzbekistan
[5] Tashkent State Technical University, Tashkent 100095, Uzbekistan
[6] Urgench State University, Kh. Alimjan Str. 14, Ugrench 221100, Uzbekistan
[7] Kimyo International University in Tashkent, Shota Rustaveli street 156, Tashkent 100121, Uzbekistan
[8] Mamun University, Bolkhovuz Street 2, Khiva 220900, Uzbekistan
[9] Alfraganus University, Yukori Karakamish Street 2a, Tashkent 100190, Uzbekistan
[10] New Uzbekistan University, Movarounnahr Str. 1, Tashkent 100000, Uzbekistan
[11] School of Physics, Harbin Institute of Technology, Harbin 150001, People's Republic of China
[*] Author to whom any correspondence should be addressed.

E-mail: suraj.pu.edu.pk@gmail.com, suraj.math@uaf.edu.pk, javlonrayimbaev6@gmail.com, i.ibragimov@kiut.uz, sokhibjan.muminov@mamunedu.uz, a.dauletov@afu.uz and ahmadjon@astrin.uz

Keywords: complexity, dark energy, dark matter, modified gravity

Abstract

We propose a new hybrid stellar model whose matter distribution is characterized by two components: normal matter and strange-quark matter. The construction of this gravitationally bound hybrid star involves a complexity-free condition, which is used to derive the temporal metric function. However, for the radial metric function, the well-known Finch-Skea metric potential is considered. To elaborate on the interplay between the matter variables of the complexity-free hybrid star, we employ the popular MIT bag model. We analyze the physical effectiveness of the complexity-free hybrid astrophysical configuration by constructing closed-form analytical solutions and then performing a complete graphical analysis to capture the model's physical features. This is achieved by considering six model stars as prospective models for strange quark-matter self-gravitating systems, such as Her X-1, SMC X-4, Vela X-1, 4U 1538-52, PSR J1614-2230, and Cen X-3. We show that the proposed hybrid stellar model is robust for accurately estimating the measured radii of the above-mentioned astrophysical configurations. In addition, several physical tests have been performed to ensure the applicability and physical consistency of the suggested model. In these tests, both analytical and graphical evaluations are included, which involve the analysis of several factors, including physically acceptable behaviors of structural variables, the equilibrium of external forces, the mass-to-radius ratio, energy bounds, gravitational redshift, and related quantities. Our findings indicate that the presented hybrid star model fulfills the required physical constraints for an astrophysically valid compact system.

1. Introduction

One of the primary areas of interest for researchers in stellar physics and cosmic science is exploring the strange features and outcomes of relativistic gravitational collapse in astrophysically dark stellar systems. These astronomical entities are produced during the final phase of stellar processes. Although there are numerous indications that compact objects are extremely dense and have a small radius, their precise nature is still unclear. Astrophysical stellar systems are classified into several groups based on their compactness factor, involving

© 2025 IOP Publishing Ltd. All rights, including for text and data mining, AI training, and similar technologies, are reserved.

quark stars, black holes, ultracompact stars, neutron stars, and white dwarfs [1]. The nature of these self-gravitating compact systems can be determined by constructing the closed-form or numerical solutions of the stellar structure equations based on Einstein's or other gravitational models. In this pursuit, the first relativistic closed-form stellar solution describing the slowly evolving, self-gravitating spherical system with isotropic matter content was proposed by Schwarzschild. Oppenheimer and Volkoff [2] investigated the balance of gravitational interactions in stellar-mass neutron stars (NS) using the static self-gravitating stellar model proposed by Tolman [3]. Many notable researchers in astrophysics have made significant contributions in the analysis of geometrically deformed high-density astrophysical bodies and black holes in Einstein's model, as well as in other higher-curvature models of gravitation [4–7].

Highly dense astrophysical objects, such as stellar-massive NS, are considered extremely fascinating cosmic elements across various scientific domains and study areas, such as quantum nuclear physics [8], astrophysical nuclear science [9], and relativistic gravitation [10]. This can be attributed to the results of extensive research into their interior characteristics and the identification and exploration of intricate processes within their structures. The groundbreaking discovery of heavily compact NS and NS mergers has sparked renewed interest in this field of study [11, 12]. The results have provided evidence for the identification of two NS, each possessing a mass of approximately two solar masses [13, 14]. The possible existence of strange matter in massive NS has been the subject of numerous studies [15]. The stellar NS are cosmic laboratories, allowing us to explore the densest matter known to exist (with a density in the range of $\approx 10^{15} - 10^{17}\,\mathrm{kg\,m^{-3}}$). Recent LIGO/Virgo gravitational wave discoveries have made these celestial bodies even more fascinating [16]. Hence, NS can be regarded as ideal cosmic objects for investigating higher-curvature gravitational models and nonconventional physics.

It is believed that SQS are completely composed of deconfined strange-quark matter [9]. On the other hand, hybrid stars usually have a core of deconfined quark matter surrounded by an outer shell of hadronic (baryonic) matter [17]. A phase transition layer separates these regions, and depending on the underlying physical assumptions, this layer may be a mixed phase (represented by a Gibbs construction) or a sharp boundary (described by a Maxwell construction). The hypothesized gravitationally compact systems known as SQS fall into the category of ultra-dense neutron stars. The presence of strange matter in stellar distributions was initially suggested by Itoh [18]. Expanding on this investigation, Bodmer [19] pointed out that the SQS, regulated by up, down, and strange quarks, exhibits greater stability than ordinary matter. These stars may consist entirely or partially of exotic quark matter, challenging the limits of our understanding of matter. By introducing the interaction between strange quark matter and baryonic matter, we can unravel the mysteries behind the development of gravitationally bound strange configurations. In this regard, Alford [20] suggested that conditions of sufficiently high density and low temperature within NS cores could lead to the compression of hadrons into quark matter. Strong evidence suggests that NS can rapidly transform into SQS via a violent deflagration, transforming nearly the entire star in mere milliseconds [21]. On the other hand, the authors of [22] examined the dynamical behavior and various structural features, along with observational consequences of SQS, that could differentiate them from NS. When the matter density in the quark matter stellar distribution approaches extremely high values, the quark-gluon separation phase occurs. These fascinating objects, known as hybrid stars, feature an intriguing structure with a hadronic outer layer enclosing a core composed of quark matter or a combination of both [23–28]. By solving the hydrostatic equilibrium relation and utilizing an equation of state (EoS) that integrates our theoretical knowledge of dense matter, one can compute the mass of a NS. The combination of hadronic and strange matter within their individual theoretical frameworks gives rise to the hybrid EoS. Although considerable progress has been achieved in the atomic-scale framework for the nucleonic EoS [29–31], the mystery of quark matter at extreme densities persists, as a definitive EoS, crucial for neutron star models, remains elusive.

Isotropy is a common assumption to model the interiors of gravitationally bound systems. Generally, no gravitationally compact stellar object displays the characteristics of a purely isotropic or perfect fluid. Therefore, the incorporation of unequal principal stresses (anisotropic pressure) is equally crucial for the construction of realistic representations of gravitationally confined configurations. According to Ruderman's studies, if the matter density associated with a gravitationally confined system exhibits higher values (i.e., $>10^{15}\mathrm{g\,cm^{-3}}$), then the compact configuration becomes anisotropic in nature [32]. These findings suggest that the radial (P_r) and tangential (P_t) pressures may differ in such highly dense self-gravitational stars. The term anisotropic pressure signifies a physical situation $P_r \neq P_t$. Anisotropic pressure naturally occurs in boson stars, hypothetical astrophysical compact systems of dense matter formed through the interaction between a complex scalar field and the gravitational field. In the same manner, the stress-energy tensor corresponding to fermionic and electric fields is anisotropic. Local anisotropy is observed to significantly influence the structural properties of gravitationally compact systems [33–41]. Different physical phenomena and high-density regimes cause the pressure to split in different directions, leading to pressure anisotropy [42]. Unequal principal stresses may arise in the stellar systems undergoing exotic phase transitions, type-P superfluid, the geometry of the π^- modes, solid cores, and boson stars (see [42] and references therein). Additionally, several notable investigations into the

dynamics of stellar configurations have been conducted under various conditions, incorporating extra degrees of freedom [43–52]. Pressure anisotropy in dense-matter compact stars can arise from various sources, especially in extreme environments. At incredibly high densities, such as those found in the cores of self-gravitating compositions, interactions between fundamental particles like quarks, baryons, and leptons can create a non-uniform distribution of pressure. This anisotropy happens because these particles can have different interaction cross-sections, varied mean free paths, or undergo condensation processes. Anisotropic pressure components may arise from the formation of color superconductivity or superfluidity in hybrid configurations and quark matter phases, particularly in the presence of strong pairing interactions. Strong internal magnetic fields or differential rotation can enhance anisotropic effects through directional stress contributions. However, this lies beyond the scope of the present investigation. Theoretical investigations suggest that certain quark matter phases might form non-uniform structures. This inherent structural arrangement can naturally lead to anisotropic pressure tensors within the material.

We can examine unequal principal stresses in terms of another physical quantity that captures the characteristics of stellar bodies, involving both anisotropic pressure and density gradients. This quantity is termed the complexity factor. Significant work has been done to formulate a well-defined interpretation of structural complexity across various scientific disciplines [53–55]. Despite these attempts, an unambiguous description characterizing the true meaning of complexity has not been achieved. Scientists have tried to capture complexity in various ways, often using concepts like information and entropy. The goal is to measure something fundamental about the structure of the system. In the context gravitationally bound systems with spherical symmetry, such as NS and white-dwarf structures, the notion of complexity based on the formalism proposed by López-Ruiz and his coworkers has been employed previously [56–58]. A generalized definition capturing the complexity of gravitationally compact objects was proposed in [19] for both the static [59] and non-static [60] spherical cases, addressing the two shortcomings of the previous definition. The novel definition is interesting due to the involvement of the fluid's pressure and matter density. However, the previously developed notions of complexity lack some essential fluid variables, including matter density and stress. This formulation is rooted in the basic assumption that a compact configuration governed by a uniform and perfect fluid corresponds to a complexity-free structure. By using this as the basis for zero complexity, the notion of complexity derives from the development of the basic framework for gravitationally strange stellar systems in general relativity. This functions similarly to an EoS that leads to the closure of Einstein's stellar structure equations when a value for the complexity factor (Y_{TF}) is set (for instance, $Y_{TF}=0$). The variable that measures complexity, Y_{TF}, originates from the orthogonal decomposition of the Riemann-Christoffel tensor.

The term Y_{TF} was introduced as a key measure for determining the structural complexity of spherically symmetric and static compact stars of dense matter. This proposal arises because Y_{TF} explicitly incorporates the terms of pressure anisotropy and density gradient. These are key parameters for capturing the physical characteristics of anisotropic stellar configurations, including neutron stars and strange matter structures. Mathematically, Y_{TF} can be defined as

$$Y_{TF} = \underbrace{8\pi\Pi}_{\text{Anisotropy}} - \underbrace{\frac{4\pi}{r^3}\int_0^r [\sigma^{eff}(y)]' y^3 dy}_{\text{Density}\quad\text{Inhomogeneity}}, \tag{1}$$

which clearly signifies the role of Y_{TF} in capturing the physical features, such as pressure anisotropy and density inhomogeneity associated with compact stars. In equation (1), $\sigma^{eff}=\sigma(y)+\sigma^{q}$, which characterizes the contribution of quark matter in the definition of Y_{TF}. The authors of [61] demonstrated that an array of equations characterizing the composition and evolution of compact spherical stars with anisotropic fluid content can be defined in terms of five scalar functions. Moreover, they showed that these scalar functions can be used to formally define all possible solutions to Einstein's equations in static scenarios. Their study revealed that Y_{TF} is one of these scalar functions, which defines the impact of density inhomogeneity on the active gravitational masses of relativistic compact stars. The condition $Y_{TF}=0$ indicates a state of the system in which the combined contributions of anisotropy and density inhomogeneity reduce to a balanced configuration. However, we emphasize that $Y_{TF}=0$ is not meant to take the place of the conventional EoS, but rather serves as an additional constraint that enhances the EoS and provides information about the structural characteristics of the system. In particular:

- **Structural Role**: Condition $Y_{TF}=0$ represents a balanced anisotropie scenario, leading to a simplified and potentially stable configuration. This implies that this constraint can significantly influence the stability and development of relativistic structures.
- **Relation to EoS**: The EoS defines the thermodynamic relationship between pressure and density within the compact configuration. In contrast, the condition $Y_{TF}=0$ governs the spatial distribution of anisotropy within the stellar interior.

To describe the thermodynamic state of the matter in neutron stars, the conventional EoS is essential since it establishes the connection between physical variables, such as matter density and pressure. On the other hand, $Y_{TF} = 0$ results from the physical and geometric framework of classical GR equations. It places a requirement on the anisotropic pressure components, which has an indirect effect on the structure, but it does not directly dictate the thermodynamic characteristics. We employed $Y_{TF} = 0$ as a heuristic constraint to discover exact analytical solutions to Einstein equations for anisotropic relativistic configurations. Recently, there have been several applications of the condition $Y_{TF} = 0$, including gravitational decoupling [62], dark energy stars [63] black holes [7], gravitational cracking [64], and the evolution of anisotropic stellar configurations [65].

The fundamental motivation for employing 'complexity-free' features in the modeling of self-gravitating stellar configurations, particularly compact stars, lies in the need to obtain closed-form solutions of the gravitational field equations. Complexity-free criteria often simplify an intricate gravitational system into a more manageable set of ordinary differential equations or algebraic relations. This enables the construction of analytical solutions that offer fundamental understanding of the astrophysical structures without relying on intensive numerical computations. Simplified analytical models reveal key relationships between internal physical features of compact stars and their observable behaviors, offering a useful framework for guiding numerical simulations and interpreting data. Models with zero complexity provide an approachable framework for studying fundamental aspects of compact stars, such as the occurrence of maximum masses, the function of anisotropic stresses, and the relevance of certain EoS.

This study models the hybrid star using an effective EoS that describes a continuous mixing of baryonic and strange-quark matter within its interior. This phenomenological approach offered mathematical tractability, enabling a qualitative study of the gravitational and structural behavior of compact stars with a nontrivial matter composition in our theoretical framework. There is a series of astrophysical studies focusing on the modeling of hybrid self-gravitating stars with anisotropic fluid distribution by employing the MIT bag model in Einstein's as well as modified gravitational models. These studies highlight the role of the MIT bag model in developing analytical solutions characterizing anisotropic hybrid stars [66–70].

It is believed that the mixed phase, depending on its existence, would only appear across a restricted density spectrum. This is particularly important in the case of a sharp first-order phase transition, as there may be no mixed phase and a discontinuous jump in density at the transition point. Since the MIT bag model is widely used as an initial approach in the literature and is analytically tractable, we adopted it to optimize the formalism for modeling the EoS of strange quark matter in our work. We agree that this model does not fully capture all aspects of quantum chromodynamics (QCD), but it is still a valuable phenomenological tool for studying the principal features of stellar configurations. To facilitate analytical analysis and focus on the gravitational dynamics of such structures, we modeled the stellar interior as a continuous mixed phase of baryonic and strange-quark matter. To facilitate analytical analysis and focus on the gravitational dynamics of such structures, we modeled the stellar interior as a continuous mixed phase of baryonic and strange-quark matter. In more realistic contexts, the phase transition between baryonic and quark matter occurs at high densities, potentially leading to a sharp interface, especially as predicted by the Maxwell construction. The Gibbs construction, which allows for a continuous transition influenced by surface tension and charge screening effects, aligns more closely with the mixed-phase scenario employed in our model. However, as the reviewer rightly pointed out, the presence and extent of such a mixed-phase region are highly sensitive to these physical parameters. It is important to note that more realistic descriptions of phase transitions in hybrid stars typically use either the Maxwell or Gibbs constructions, depending on assumptions about surface tension and global charge neutrality [23, 71]. Our simplified method, which assumes a continuous transition without imposing a sharp interface, is more in line with the Gibbs-type treatment.

Building on the previously mentioned findings, our goal is to conduct a comprehensive analysis of how anisotropy influences the structural features of gravitational hybrid stars under the zero- complexity condition. In this article, we use the popular MIT bag model for quark matter. Numerous scientists have frequently used this model to develop SQS [72–76]. We hope that this research will make significant contributions to the field of stellar physics and cosmology, particularly in the areas of high-gravity regimes and exotic matter states. The manuscript is structured as follows: The mathematical formalism required for the gravitational field equations and the EoS for the MIT model is discussed in section 2. We also discuss the junction condition for the complexity-free hybrid star model in the same section. In section 3, we provide a fundamental formalism for developing the complexity-free stellar structure. Then, by considering the radial metric function corresponding to the Finch-Skea model, we formulate the temporal counterpart in section 4. Subsequently, the anisotropic solution with complexity-free characterization is developed using the MIT bag model in the same section. In section 5, we explore the conditions of physical acceptability and stability constraints, along with key physical properties necessary for the realistic modeling of strange stellar structures. Finally, section 6 presents a summary of the results, accompanied by a comprehensive discussion and future directions for the work.

2. The general formalism

Einstein's gravitational model connects the distribution of material content and energy with the geometric structure of spacetime, and conversely, the spacetime geometry influences the motion of matter and energy. The interrelated nature of matter, energy, and spacetime is represented mathematically using a tensorial formalism.

$$G_{\mu\nu} \equiv R_{\mu\nu} - \frac{1}{2}g_{\mu\nu}R = 8\pi T^{(eff)}_{\mu\nu}, \tag{2}$$

Here, the tensorial term $R_{\mu\nu}$ symbolizes the Ricci tensor, while the scalar term R represents the curvature scalar. These factors are determined using the metric tensor $g_{\mu\nu}$, which captures the geometric features of spacetime. For simplicity, we adopt a system of units where the gravitational constant (G) and speed of light (c) are defined as unity. The matter-energy content is defined by the stress tensor $T^{eff}_{\mu\nu}$ with energy density σ^{eff} and stress components P^{eff}_r (radial) and P^{eff}_t (tangential) as

$$T^{\mu}{}_{\nu} = \text{diag}(\sigma^{eff}, -P^{eff}_r, -P^{eff}_t, -P^{eff}_t). \tag{3}$$

For a static, spherical relativistic matter distribution with differentiable geometric variables $e^{\nu(r)}$ and $e^{\lambda(r)}$, the interior Schwarzschild metric reads

$$ds^2 = e^{\nu(r)}dt^2 - e^{\lambda(r)}dr^2 - r^2(d\theta^2 + \sin^2\theta d\phi^2). \tag{4}$$

Next, we define the effective stress-energy tensor $T^{eff}_{\mu\nu}$ as

$$T^{eff}_{\mu\nu} = T_{\mu\nu} + T^{q}_{\mu\nu}, \tag{5}$$

where the component $T_{\mu\nu}$ of the stress tensor characterizes the distribution of baryonic matter, the gravitational source, which is modeled as anisotropic to account for the influence of the surrounding matter, as commonly observed in standard astrophysical structures. This component shows how pressure gradients, rotation, and strong interactions cause gravitationally compact systems to deviate from the isotropic regime. However, component $T^{q}_{\mu\nu}$ characterizes the distribution of quark matter, which is described by a specific EoS. This element captures the interactions and thermodynamic features of quark matter in highly dense environments, such as the cores of hybrid stellar structures [77]. The terms $T_{\mu\nu}$ and $T^{q}_{\mu\nu}$ are defined as

$$T^{\mu(eff)}_{\nu} = \text{diag}(\sigma, -P_r, -P_t, -P_t), \tag{6}$$

$$T^{\mu(q)}_{\nu} = \text{diag}(\sigma^q, -P^q, -P^q, -P^q), \tag{7}$$

respectively. Consequently, the non-zero null mathematical terms associated with Einstein's gravitational equations read

$$G^{t}{}_{t} = 8\pi T^{t(eff)}_{t} : \frac{1}{r^2} - \left(\frac{1}{r^2} - \frac{\lambda'}{r}\right)e^{-\lambda} = 8\pi\sigma^{eff}, \tag{8}$$

$$G^{r}{}_{r} = 8\pi T^{r(eff)}_{r} : -\frac{1}{r^2} + \left(\frac{1}{r^2} + \frac{\nu'}{r}\right)e^{-\lambda} = 8\pi P^{eff}_r, \tag{9}$$

$$G^{\theta}{}_{\theta} = 8\pi T^{\theta(eff)}_{\theta} : \frac{1}{4}\left[2\nu'' + \nu'\left(\nu' - \lambda' + \frac{2}{r}\right) - 2\frac{\lambda'}{r}\right]e^{-\lambda} = 8\pi P^{eff}_t, \tag{10}$$

where $f' := \partial_r$. The stress tensor corresponding to the two-fluid model can be expressed as

$$T^{t(eff)}_{t} \equiv \sigma^{eff} = \sigma + \sigma^q, \tag{11}$$

$$T^{r(eff)}_{r} \equiv -P^{eff}_r = -(P_r + P^q), \tag{12}$$

$$T^{\theta(eff)}_{\theta} = T^{\phi(eff)}_{\phi} \equiv -P^{eff}_t = -(P_t + P^q), \tag{13}$$

$$T^{\mu(eff)}_{\nu} = 0, \quad \text{with} \quad \mu \neq \nu. \tag{14}$$

In the above set of equations (11)–(14), σ^q, P^q_r, and P^q_t denote the energy density and principal stresses associated with the quark matter, respectively. The MIT bag model EoS [22, 78] governs the pressure-density relationship for quark matter, which is expressed as

$$P^q = \frac{1}{3}(\sigma^q - 4B_g), \tag{15}$$

where B_g denotes the bags constant. The MIT bag model has commonly been employed to model the distribution of quark matter within static, spherical stellar compositions, such as quark stars and neutron stars [79–81]. In its most basic version, the MIT bag model usually considers quarks to be free particles trapped in a bag with a given vacuum energy density (B_g). It lacks an inherent mechanism to account for dynamical chiral

symmetry breaking, which is a fundamental aspect of QCD at low to moderate densities. However, quark-quark interactions responsible for dynamical chiral symmetry breaking and its restoration at higher densities are explicitly incorporated in the Nambu-Jona-Lasinio (NJL) model [82]. This can significantly influence the EoS and the properties of quark matter. In the traditional MIT bag model, quarks are assumed to have fixed, tiny current masses that are contained within the bag. In contrast, the NJL model includes dynamically produced quark masses that fluctuate with density and temperature, providing a more accurate description of quark behavior in severe situations. A non-perturbative vacuum pressure, represented by the bag constant B_g, is used in the MIT bag model to parameterize confinement. Although it provides a simplified view of the intricate, non-perturbative interactions between quarks and gluons, it is effective in explaining some elements of hadron spectroscopy. Despite being a theoretical framework, the NJL model includes effective quark-quark interactions that may replicate scalar and pseudoscalar interactions, two features of the fundamental mechanics of QCD. Color superconducting phases of quark matter at large densities can be predicted by extending the NJL model to incorporate diquark pairing interactions. The cooling and transport characteristics of compact stars are significantly impacted by these phases. Color superconductivity must be provided as an additional component because it is not inherent in the fundamental MIT bag model.

The choice of the bag constant B_g in the MIT bag model, which characterizes the quark matter phase, has a significant impact on the predicted properties of hybrid stars, particularly their mass-radius relation and stability. In general, lower values of B_g yield a stiffer equation of state (EoS) for quark matter, allowing hybrid stars to sustain higher maximum masses. Conversely, higher values of B_g typically produce a softer EoS, leading to lower maximum masses. This occurs because a larger bag constant increases the vacuum energy contribution, making quark matter less bound and thus effectively softer. The influence of B_g on the stellar radius is more nuanced and can vary depending on the specific mass range, the properties of the hadronic equation of state, and the nature of the phase transition.

- A softer quark matter EoS, associated with higher values of B_g, can cause low-mass stars to exhibit reduced radii due to the increased central density needed to balance pressure gradients.
- This tendency may change near the maximum mass, with models featuring different bag constants showing variations in the corresponding stellar radius.

The dynamics of phase transitions between the hadronic and quark matter phases and the compressibility of these phases have a crucial impact on the stability and equilibrium of hybrid stars. The stability of the resulting hybrid star is indirectly influenced by B_g through its effect on the quark matter EoS. For instance, an extremely soft quark matter EoS may lead to unstable configurations following the phase transition.

We employ an additional constraint within the context of normal matter. According to this constraint, the radial pressure associated with normal matter is considered proportional to its energy density, that is,

$$P_r = m\sigma, \tag{16}$$

where m is the EoS parameter, with $m \in (0, 1)$ and $m \neq \frac{1}{3}$.

The mass of a relativistic, spherical astrophysical compact configuration has the form

$$M^{eff}(r) = \frac{r}{2}(1 - e^{-\lambda}), \tag{17}$$

which can alternatively be expressed as

$$\frac{M^{eff}}{dr} = 4\pi r^2 \sigma^{eff} \Rightarrow M^{eff} = 4\pi \int_0^r \sigma^{eff}(y) y^2 dy. \tag{18}$$

The above relation may be defined via energy density of normal matter plus the energy density of quark matter as

$$M^{eff} = 4\pi \int_0^r \sigma(x) y^2 dy + 4\pi \int_0^r \sigma^q(y) y^2 dy, \tag{19}$$

$$M^{eff} = M^s + M^q, \tag{20}$$

where the mass functions corresponding to regular matter and quark matter are denoted by M^s and M^q, respectively. The metric describing the geometry of the Schwarzschild outer spacetime is defined as

$$ds^2 = f(r)dt^2 - \frac{dr^2}{f(r)} - r^2(d\theta^2 + \sin^2\theta d\phi^2), \tag{21}$$

where $f(r) = 1 - \frac{2M}{r}$, with M representing the mass corresponding to the hybrid stellar structure. Next, the continuity of the geometric variables g_{00} and g_{11} and $\frac{\partial g_{00}}{\partial r}$ at the stellar surface $r = r_\Sigma$ yields

$$\text{Continuity of } g_{tt}: \quad e^{\nu_\Sigma} = \left(1 - \frac{2M}{r_\Sigma}\right), \tag{22}$$

$$\text{Continuity of } g_{rr}: \quad e^{\lambda_\Sigma} = \left(1 - \frac{2M}{r_\Sigma}\right)^{-1}, \tag{23}$$

$$\text{Continuity of } \frac{dg_{rr}}{dr}: \quad \left[\frac{de^{\lambda}}{dr}\right]_\Sigma = \frac{2M}{r_\Sigma^2}, \tag{24}$$

$$\text{Vanishing of pressure}: \quad [P_r]_\Sigma = 0, \tag{25}$$

where the subscript Σ shows that the quantity is measured on the boundary of gravitational compact system.

3. Complexity-free relativistic framework

The authors of [61] developed certain mathematical scalar components of the Riemann tensor $R_{\mu\nu\epsilon\omega}$ that emerge as a result of the orthogonal splitting of $R_{\mu\nu\epsilon\omega}$. These fragments of $R_{\mu\nu\epsilon\omega}$ have proven to be vital in exploring the physical features of astrophysical stellar structures [59, 60, 83]. These scalar terms are essential to this investigation, as the mathematical term used to gauge the gravitational complexity in astrophysical compact entities is a trace-free term of $R_{\mu\nu\epsilon\omega}$. The modified form of Y_{TF} has been explored by several researchers within the context of slowly evolving and dynamical spherical stellar distributions by considering different gravitational models [34, 84]. The true significance of this definition becomes apparent when it is used as an additional constraint to solve the gravitationally compact systems. In this respect, the authors of the studies [85–87] have shown that the notion of Y_{TF} can be employed to explore the impacts of gravitational decoupling on the structure of astrophysically dark objects. Additionally, some studies have also discussed the generic astrophysical features of stellar objects by employing a complexity-free scheme [5, 88, 89]. To formulate the expression for complexity factor, we begin by defining the electric part of $R_{\mu\nu\epsilon\omega}$, which has a particular mathematical form (see [59] for details). The orthogonal splitting formalism yields the following tensorial terms

$$Y_{\mu\nu} = R_{\mu\varepsilon\nu\omega}U^{\varepsilon}U^{\omega}, \tag{26}$$

$$Z_{\mu\nu} =^{*} R_{\mu\varepsilon\nu\omega}U^{\varepsilon}U^{\omega}, \tag{27}$$

$$X_{\mu\nu} =^{*} R^{*}_{\mu\varepsilon\nu\omega}U^{\varepsilon}U^{\omega}, \tag{28}$$

where U^{μ} denotes the four-velocity and * represents the dual tensor, i.e., $R^{*}_{\mu\nu\varepsilon\omega} = \frac{1}{2}\eta_{\epsilon\gamma\varepsilon\omega}R_{\mu\nu}{}^{\epsilon\gamma}$, with $\eta_{\epsilon\gamma\varepsilon\omega}$ being the Levi-Civita tensor. Then, using the Einstein field equations with anisotropic matter distribution, Riemann tensor can be defined as (see [59] for details)

$$R^{\mu\varepsilon}{}_{\nu\omega} = C^{\mu\epsilon}{}_{\nu\omega} + 28\pi T^{[\mu}{}_{[\nu}\delta^{\varepsilon]}{}_{\omega]} + 8\pi T\left(\frac{1}{3}\delta^{\mu}{}_{[\mu}\delta^{\varepsilon}_{\omega]} - \delta^{[\mu}{}_{[\mu}\delta^{\varepsilon]}{}_{\omega]}\right), \tag{29}$$

where T is the trace of stress-energy tensor. The above expression can be decomposed as

$$R^{\mu\varepsilon}{}_{\nu\omega} = R^{\mu\epsilon}{}_{(I)\nu\omega} + R^{\mu\epsilon}{}_{(II)\nu\omega} + R^{\mu\varepsilon}{}_{(III)\nu\omega}, \tag{30}$$

where

$$R^{\mu\varepsilon}{}_{(I)\nu\omega} = 16\pi\sigma^{eff}U^{[\mu}U_{[\nu}\delta^{\epsilon]}{}_{\omega]} + 28\pi Ph^{[\mu}{}_{[\nu}\delta^{\epsilon]}{}_{\omega]} + 8\pi(\sigma^{eff} - 3P)\left(\frac{1}{3}\delta^{\mu}{}_{[\mu}\delta^{\varepsilon}{}_{\omega]} - \delta^{[\mu}{}_{[\mu}\delta^{\varepsilon]}{}_{\omega]}\right), \tag{31}$$

$$R^{\mu\varepsilon}{}_{(II)\nu\omega} = 16\pi(\Pi\delta^{[\mu}{}_{[\mu}\delta^{\varepsilon]}{}_{\omega]}), \tag{32}$$

$$R^{\mu\varepsilon}{}_{(III)\nu\omega} = 4U^{[\mu}U_{[\nu}E^{\varepsilon]}{}_{\omega]} - \xi^{\mu\varepsilon}{}_{\lambda}\xi_{\nu\omega\rho}E^{\lambda\rho}, \tag{33}$$

where $P = (P_r + 2P_t)/3$, $h_{\mu\nu} = g_{\mu\nu} + U_{\mu}U_{\nu}$ is the projection tensor, $E_{\mu\nu}$ denotes the electric part of Weyl tensor, and

$$\xi_{\mu\varepsilon\nu} = U^{\lambda}\eta_{\lambda\mu\varepsilon\nu}, \quad \xi_{\mu\varepsilon\nu}U^{\nu} = 0, \tag{34}$$

where we have used the fact that magnetic part of Weyl tensor ($H_{\mu\nu} = {}^{*}C_{\mu\varepsilon\nu\omega}U^{\varepsilon}U^{\omega}$) vanishes in case of spherical symmetry. Then, consequently, the tensor $Y_{\mu\nu}$ can be expressed as

$$Y_{\mu\nu} = \frac{4\pi}{3}(\sigma^{eff} + 3P)h_{\mu\nu} + 4\pi\Pi_{\mu\nu} + E_{\mu\nu}, \tag{35}$$

which may be defined in terms of its trace (Y_T) and trace-free (Y_{TF}) components as

$$Y_{\mu\nu} = \frac{1}{3}Y_T h_{\mu\nu} + Y_{TF}\left(\mathcal{X}_\mu\mathcal{X}_\nu - \frac{1}{3}h_{\mu\nu}\right), \tag{36}$$

where $h_{\mu\nu} = g_{\mu\nu} + U_\mu U_\nu$ is the projection tensor and $\mathcal{X}_\mu$ represents the unit four vector. The scalar terms Y_T and Y_{TF} are defined as

$$Y_T = 4\pi(\sigma^{eff} + 3P_r^{eff} - 2\Pi^{eff}), \quad Y_{TF} = 4\pi\Pi + E. \tag{37}$$

Here, $\Pi^{eff} = P_t^{eff} - P_r^{eff}$ is the anisotropic scalar and E is Weyl scalar. The scalar Y_{TF} can be defined in terms of energy density of the stellar structure as

$$Y_{TF} = 8\pi\Pi - \frac{4\pi}{r^3}\int_0^r [\sigma^{eff}(y)]' y^3 dy, \tag{38}$$

$$Y_{TF} = 8\pi(P_t - P_r) - \frac{4\pi}{r^3}\int_0^r [\sigma(y) + \sigma^q(y)]' y^3 dy. \tag{39}$$

On substituting the values of matter variables, we get

$$Y_{TF} = \frac{\nu'[r(\lambda' - \nu') + 2] - 2r\nu''}{4re^{\lambda(r)}}. \tag{40}$$

Then, by employing the complexity-free constraint ($Y_{TF} = 0$), we have

$$2r\nu'' - (r\lambda' - r\nu' + 2)\nu' = 0, \tag{41}$$

which upon integrating and rearranging provides the following result

$$e^{\nu(r)} = \left(A\int_0^r re^{\lambda/2}dr + B\right)^2, \tag{42}$$

where the terms A and B are integration constants. In this respect, the following points are worth noting:

- The scalar T_{TF} vanishes not only for astrophysical stellar systems with uniform density and pressure but also in scenarios where these factors counterbalance each other.
- The previous point implies that numerous astronomical compact configurations may satisfy the condition $Y_{TF} = 0$.
- It is important to point out that, for any relativistic stellar system, anisotropic pressure contributes locally to $Y_{TF} = 0$, while the non-uniformity of energy density contributes non-locally.
- If the astrophysical fluid configuration involves electric charge, then the associated Y_{TF} will comprise both local and non-local contributions from the electric field.

4. Modeling hybrid stars under the condition $Y_{TF} = 0$

We aim to develop well-behaved astrophysical stellar solutions that describe complexity-free hybrid stars by analytically solving Einstein's gravitational equations for static, spherically confined distributions. This task is challenging due to the non-linearity of the gravitational system of equations, and different astrophysical approaches are commonly used to address it. Here, we construct an explicit metric potential based on the Finch and Skea (FS) ansatz [90], which is often used for modeling astrophysical stellar structures. This metric ansatz was employed by Duorah and Ray in the context of stellar structures [91]. They pointed out that this kind of ansatz may not be compatible with the stellar structure equations characterizing the interior configuration of compact gravitational entities. The development of astronomical compact systems has been significantly impacted by this specific form of the FS ansatz, as its outcomes are widely accepted and meet all essential requirements for physical feasibility [92]. This ansatz has been widely studied in both Einstein's model and modified gravitational models due to its astrophysical and cosmological applications [62, 93–96]. Inspired by the previous discussion, we consider the radial component of FS perfect metric, given by

$$g_{rr} = e^{\lambda(r)} = 1 + Sr^2, \tag{43}$$

where S is a constant of integration with units of $[length^{-2}]$. The FS metric is a well-known analytical solution to Einstein's field equations for a spherically symmetric, anisotropic fluid distribution. Its key benefits are that it is mathematically tractable and yields physically plausible profiles for density, pressure, and anisotropy. It also ensures vanishing pressure at the surface and remains regular at the core, making it well-suited for modeling static, spherical matter compositions. The choice of this metric stems from its analytical tractability, which is

crucial for developing closed-form solutions that describe dense matter objects. However, the generality of our model is inherently limited by the use of the FS metric as an analytical solution. Since it represents a specific functional form of the metric potentials, it may not fully capture the complex interior structures that could arise from arbitrary EoS. The metric accepts anisotropic pressure and meets regularity requirements because of its unique structure, but it does not allow for total freedom in choosing the equation of state. Rather of being introduced independently based on basic microphysical principles, the metric determines or constrains the equation of state to some extent. In contrast to many simpler isotropic models, it automatically integrates pressure anisotropy, a critical property predicted in compact stars. Thus, although our results are valid within the context of the FS geometry, their direct quantitative applicability to all possible compact star configurations is limited.

Then, applying the complexity-free constraint (42) yields the temporal metric potential as

$$e^{\nu(r)} = \left[B + \frac{A(1+Sr^2)^{3/2}}{3S}\right]^2, \tag{44}$$

where B, and A are integration constants. These constants are calculated form the matching conditions (22)–(25). Then, by applying the radial (43) and temporal (44) metric functions to the gravitational system in equations (8)–(10), we obtain

$$8\pi(\sigma+\sigma^q) = \frac{S(3+Sr^2)}{(1+Sr^2)^2}, \tag{45}$$

$$8\pi(P_r+P^q) = -\frac{S(3BS+A(-5+Sr^2)\sqrt{1+Sr^2})}{(1+Sr^2)(3BS+A(1+Sr^2)^{3/2})}, \tag{46}$$

$$8\pi(P_t+P^q) = \frac{S(-3BS+5A(1+Sr^2)^{3/2})}{(1+Sr^2)(3BS+A(1+Sr^2)^{3/2})}. \tag{47}$$

Then, by solving equations (45)–(47) by employing equations (15) and (16), we obtain expressions for σ, P_r, and P_t corresponding to the normal matter as

$$\sigma = \frac{2A(1+r^2S)^{3/2}(S(3-r^2S)+8\pi B_g(1+r^2S)^2)+3BS(16\pi B_g(1+r^2S)^2-S(3+2r^2S))}{4\pi(3m-1)(1+r^2S)^2(3BS+A(1+r^2S)^{3/2})}, \tag{48}$$

$$P_r = \frac{2mA(1+r^2S)^{3/2}(S(3-r^2S)+8\pi mB_g(1+r^2S)^2)+3mBS(16\pi B_g(1+r^2S)^2-S(3+2r^2S))}{4\pi(3m-1)(1+r^2S)^2(3BS+A(1+r^2S)^{3/2})}, \tag{49}$$

$$P_t = \frac{A(1+r^2S)^{3/2}(32\pi mB_g(1+r^2S)^2-S(r^2S+m(-12+r^2S)))+3BS(32\pi mB_g(1+r^2S)^2)}{8\pi(3m-1)(1+r^2S)^2(3BS+A(1+r^2S)^{3/2})} - \frac{3BS^2(r^2S+m(6+r^2S))}{8\pi(3m-1)(1+r^2S)^2(3BS+A(1+r^2S)^{3/2})}. \tag{50}$$

The variables associated with quark matter are defined as

$$\sigma^q = \frac{-A(1+r^2S)^{3/2}(32\pi mB_g(1+r^2S)^2-3S(-5+r^2S+m(3+r^2S)))-96\pi mBSB_g(1+r^2S)^{5/2}}{8\pi(3m-1)(1+r^2S)^2(3BS+A(1+r^2S)^{3/2})} + \frac{3BS^2(1+r^2S+m(3+r^2S))}{8\pi(3m-1)(1+r^2S)^2(3BS+A(1+r^2S)^{3/2})}, \tag{51}$$

$$P^q = \frac{A(1+r^2S)^{3/2}(-32\pi mB_g(1+r^2S)^2+S(-5+r^2S+m(3+r^2S)))+3BS(-32\pi mB_g(1+r^2S)^2)}{8\pi(3m-1)(1+r^2S)^2(3BS+A(1+r^2S)^{3/2})} + \frac{3BS^2(1+r^2S+m(3+r^2S))}{8\pi(3m-1)(1+r^2S)^2(3BS+A(1+r^2S)^{3/2})}. \tag{52}$$

The anisotropic scalar associated with baryonic matter takes the following form

$$\Pi \equiv P_t - P_r = \frac{r^2S^2}{8\pi(1+r^2S)^2}. \tag{53}$$

It is notable that the factor $\frac{2\Pi}{r}$ is referred to as the anisotropic force, which is repulsive for $\Pi > 0$ and attractive for $\Pi < 0$. The behavior of anisotropic scalar is shown in figure 3 (left panel). According to this profile, the Π exhibits positive behavior, resulting in a repulsive anisotropic force. This may lead to the emergence of more

Table 1. The numerical values of A, B, S, and B_g for different stellar structures by considering $m = 0.4$.

Compact Star	$M(M_\odot)$	R(km)	A (km^{-2})	B	S (km^{-2})	B_g (km^{-2})
Her X-1 [98]	0.85	8.5	0.00138408	0.708088	0.00346021	0.0000715922
SMC X-4 [99]	1.29	8.8	0.00189296	0.642483	0.00535629	0.0000908958
Vela X-1 [100]	1.77	9.5	0.00206444	0.581646	0.00658127	0.0000908958
4U 1538-52 [101]	0.87	7.8	0.00180283	0.573697	0.00583935	0.0000931452
PSR J1614-2230 [11]	1.97	10.3	0.00191347	0.619548	0.00566044	0.0000801591
Cen X-3 [99]	1.49	9.2	0.00191347	0.619548	0.00566044	0.0000895411

dense astrophysical systems, as examined in [97]. In addition, the scalar Π vanishes within the core of the astrophysical system, i.e., $\Pi \to 0$ as $r \to 0$, as expected for a realistic stellar model.

The value of B_g is evaluated using the condition $P_r(r = r_\Sigma) = 0$ as

$$B_g = \frac{S(2A(-3 + r_\Sigma^2 S)(1 + r_\Sigma^2 S)^2 + 3BS(3 + 2r_\Sigma^2 S)\sqrt{1 + r_\Sigma^2 S})}{16\pi(3BS + A(1 + r_\Sigma^2 S)^{3/2})(1 + r_\Sigma^2 S)^{5/2}}. \tag{54}$$

The numerical values of the B_g for different stellar systems are given in table 1. By solving the matching conditions (41)–(43), we find

$$A = \frac{M}{r_\Sigma^3}, \tag{55}$$

$$S = \frac{2M}{(r_\Sigma - 2M)r_\Sigma^2}, \tag{56}$$

$$B = \frac{1}{6}\left(5 - \frac{12M}{r_\Sigma}\right)\left(1 - \frac{2M}{r_\Sigma}\right)^{-1/2}. \tag{57}$$

We require suitable values for the constants A, B, and S to graphically illustrate the presented complexity-free hybrid star model. We calculate the values of A, B, and S for the stellar models considered, as shown in table 1.

5. Essential physical characteristics of the model

Understanding the composition and dynamics of astrophysical compact systems requires careful attention to their physical characteristics. Anisotropy, density, and pressure are key variables that influence the composition, stability, and evolution of these gravitationally confined distributions. By studying these parameters, we can uncover key understandings of extreme conditions of matter. Investigating the physical properties of strange stellar distributions enhances our understanding of both stellar and cosmological phenomena, advancing our knowledge of fundamental physics in high-density regimes.

5.1. Regularity of the geometric and physical variables

A solution for a physically acceptable stellar model should exhibit finite, positive values for the metric functions, indicating the absence of geometric and physical singularities.

$$[e^{\lambda(r)}]_{r=0} = 1, \quad [e^{\nu(r)}]_{r=0} = \left(B + \frac{A}{3S}\right)^2 > 0. \tag{58}$$

The variation of the geometric variables for the considered model stars is displayed in figure 1. It is observed that both geometric variables are well-behaved within the compact region. The central values of the density and pressure components associated with baryonic matter are defined as

$$\sigma(0) = \frac{2A(3S + 8\pi B_g) + 3BS(16\pi B_g - 3S)}{4\pi(3m - 1)(3BS + A)}, \tag{59}$$

$$P_r(0) = P_t(0) = \frac{2mA(3S + 8\pi B_g) + 3BS(16\pi B_g - 3mS)}{4\pi(3m - 1)(3BS + A)}. \tag{60}$$

According to equations (59)–(60) that the central density and pressures are finite, indicating a singularity-free model. The following factors are imperative for the model to be physically valid:

1. The gravitational fluid sphere must exhibit non-negative matter density and radial/transverse pressures, i.e, $\sigma, P_r, P_t > 0$ for $0 \leqslant r < r_\Sigma$. Furthermore, the P_r must be zero at the r_Σ, i.e., $P_r(r = r_\Sigma) = 0$.

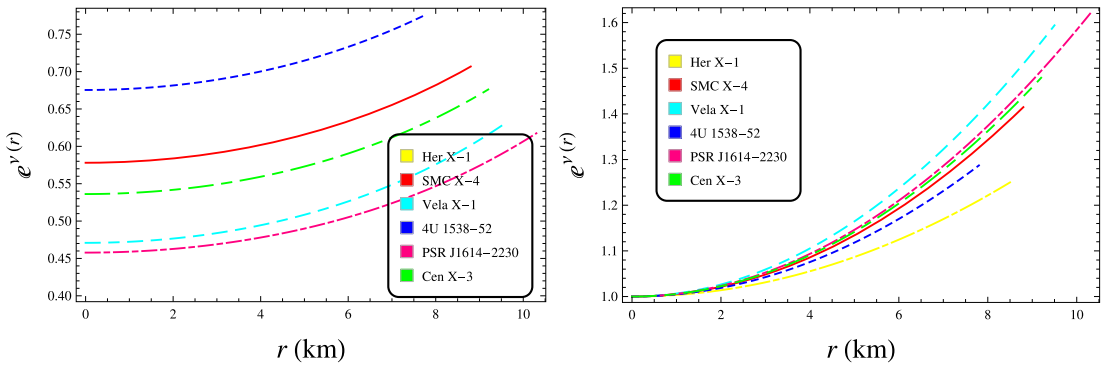

Figure 1. Plots of metric potentials versus r for the considered compact stars.

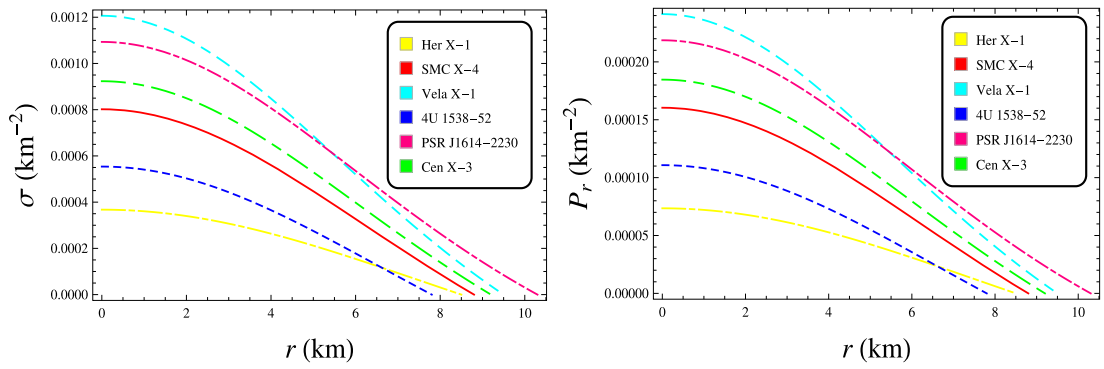

Figure 2. Plots of σ and P_r versus r for the considered compact stars.

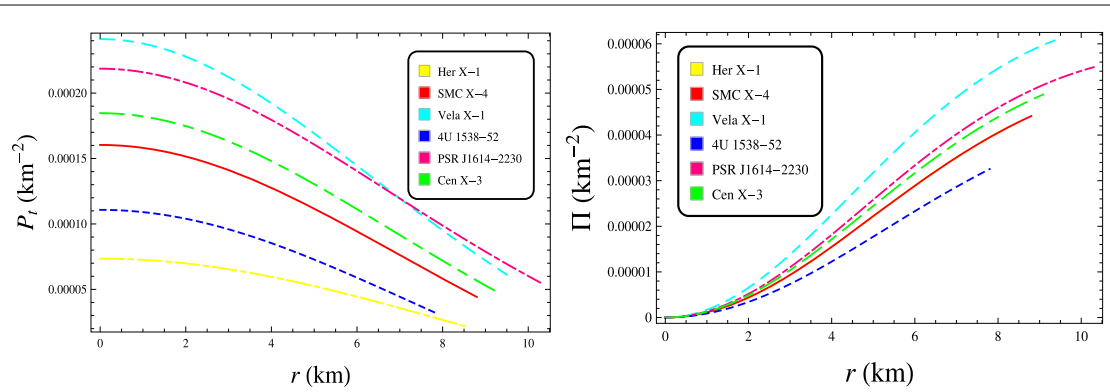

Figure 3. Variations of P_t and Π against r for the considered stellar models.

2. The terms σ and P_r should decrease monotonically with increasing r, i.e., $\frac{d\sigma}{dr} < 0$ and $\frac{dP_r}{dr} < 0$ for $0 < r < r_{\Sigma}$. The behaviors of the quantities σ, P_r, P_t, $\frac{d\sigma}{dr}$, and $\frac{dP_r}{dr}$ for the considered stellar models are described in figures 2–4. These profiles confirm that the proposed complexity-free hybrid star model satisfies the conditions of physical acceptability.

Figure 5 displays the profile of energy density and pressure associated with quark matter. The graphical representation shown in figure 5 illustrates that σ^q reaches its maximum at the center and decreases monotonically toward the boundary of the hybrid configuration, becoming zero at the interface with the hadronic envelope. This behavior is consistent with physical expectations for hybrid stars. Furthermore, the profile of p^q also adheres to physical bounds, attaining its maximum at the core and vanishing at the boundary.

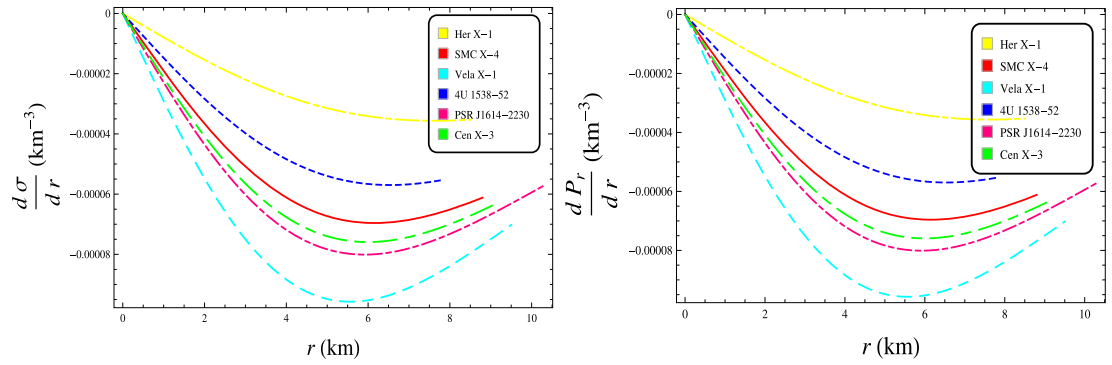

Figure 4. Plots of σ-gradient and P_r-gradient against r.

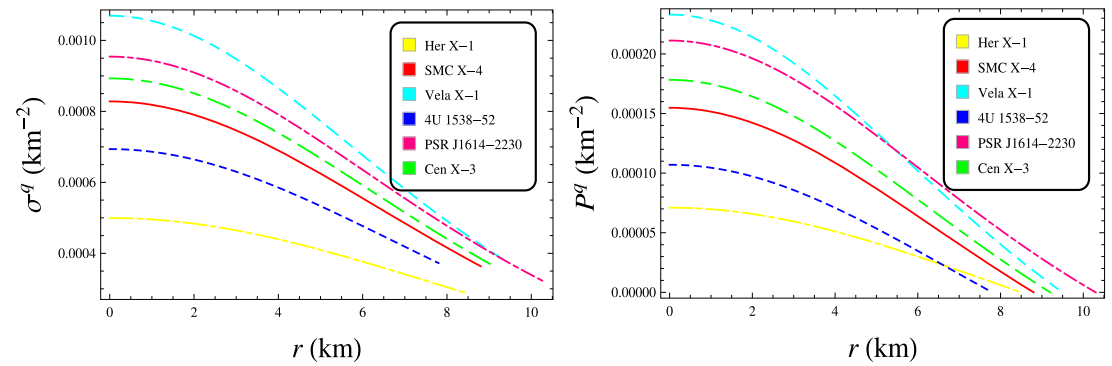

Figure 5. Plot of σ^q and p^q against r for considered compact stars.

5.2. Energy conditions

For an astrophysical compact formation to be stable and physically viable, energy conditions are one of the essential ingredients. They ensure that characteristics such as density and pressure remain non-negative by imposing fundamental restrictions on the matter-energy content of the stellar structure. By meeting these requirements, gravitationally compact entities can avoid unphysical situations, improving our understanding of their genesis, development, and ultimate destiny in space. The Weak Energy Condition (WEC), Null Energy Condition (NEC), Dominant Energy Condition (DEC), and Strong Energy Condition (SEC) are fundamental constraints that must be fulfilled by a realistic astrophysical stellar structure with anisotropic pressure. These conditions are defined through the following set of inequalities.

$$\text{(i)} \quad \text{WEC} : \sigma \geqslant 0, \quad \sigma + P_r \geqslant 0, \quad \sigma + P_t \geqslant 0, \tag{61}$$

$$\text{(ii)} \quad \text{NEC} : \sigma + P_r \geqslant 0, \quad \sigma + P_t \geqslant 0, \tag{62}$$

$$\text{(iii)} \quad \text{SEC} : \sigma + P_r + 2P_t \geqslant 0, \quad \sigma + P_r \geqslant 0, \quad \sigma + P_t \geqslant 0, \tag{63}$$

$$\text{(ii)} \quad \text{DEC} : \sigma \geqslant |P_r|, \quad \sigma \geqslant |P_t|. \tag{64}$$

The above-mentioned energy bounds are fulfilled for the proposed complexity-free hybrid stellar model, as demonstrated by figure 6, which displays the behavior of these conditions for the considered compact stars.

5.3. Hydrostatic equilibrium

In general relativity (GR), the Tolman-Oppenheimer-Volkoff (TOV) equations are the recognized standard for modeling the equilibrium of self-gravitating configurations. However, mechanisms from special relativity, which neglects gravity, is often used to construct the EoS for dense matter, such as baryonic or quark matter. In astrophysics, transitioning between these frameworks is a well-known yet challenging process. Although the quantized EoS is frequently used in nuclear physics and GR is a classical theory, astrophysics often employs the EoS in TOV equations as an approximation. The quantized EoS, when combined with the TOV equations, represents the macroscopic gravitational dynamics of stellar formation while also capturing microscopic strong interaction effects. Gravitational forces are negligible at the nuclear scale due to their size, whereas strong interactions dominate. Gravity becomes significant at the macroscopic scale (stellar level), and the EoS is used to

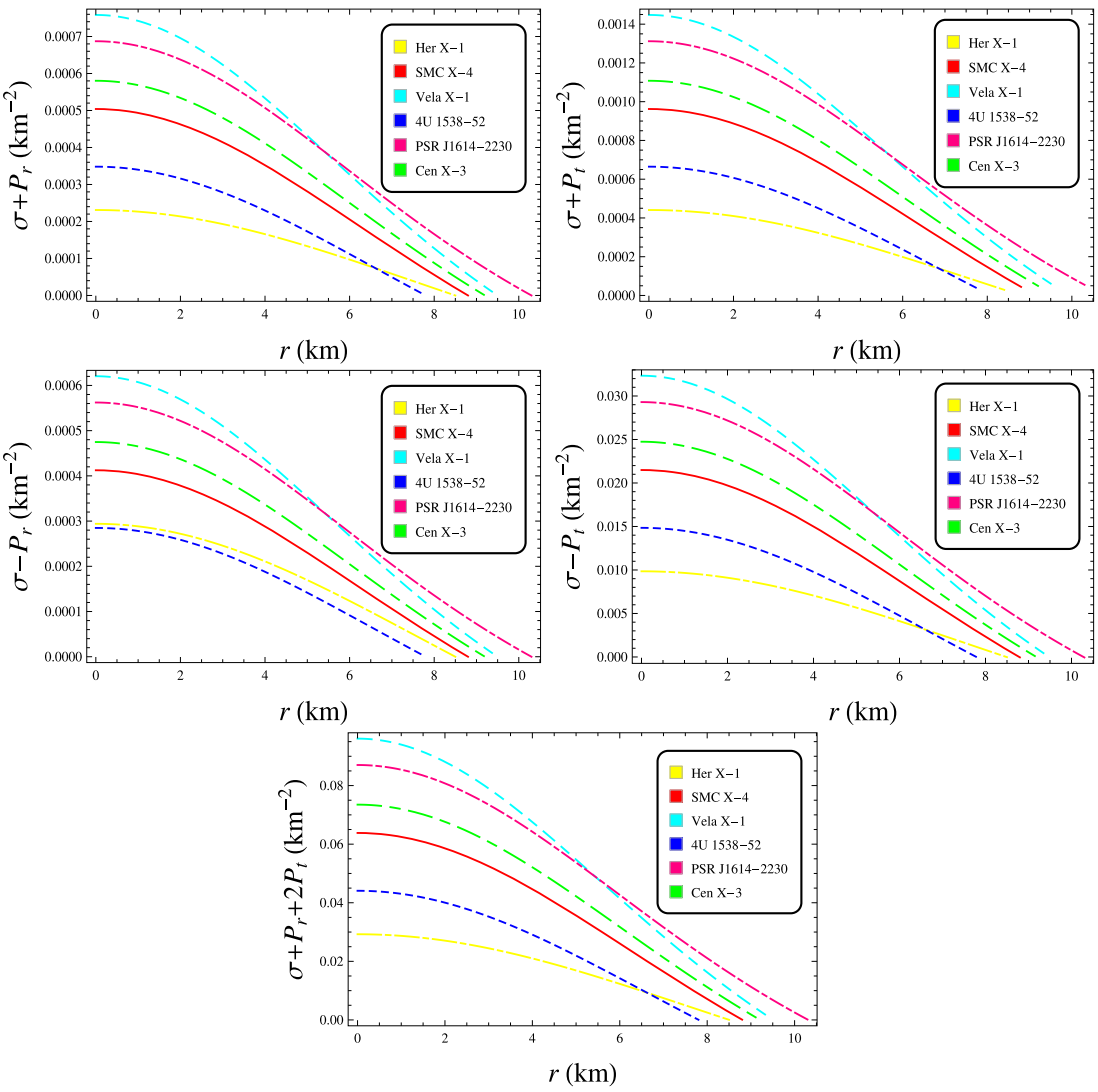

Figure 6. Graphical description of energy conditions against r.

translate microscopic physics into the global behavior described by the TOV equations. Astronomical compact objects can be described within the mixed framework, as it accounts for both macroscopic gravitational equilibrium (via the TOV equations) and microscopic strong interaction effects (through the EoS). Prior research has validated the approach, and the approximations used, such as mean-field theory, are widely acknowledged. The balance of forces (gravity, hydrostatic pressure, and anisotropic pressure) within the astrophysical compact system is governed by the generalized equation of hydrostatic equilibrium, defined as follows

$$\nabla^{\mu}T_{\mu\nu}=0\Rightarrow\quad \frac{dP_r}{dr}+\frac{\nu'}{2}(\sigma+P_r)-\frac{2}{r}(P_t-P_r)-\frac{\nu'}{2}(\sigma^q+P_r^q)-\frac{dP^q}{dr}=0, \tag{65}$$

which can be decomposed into three forces: F_h (hydrostatic), F_g (gravitational), F_a (anisotropic), and F_q (quark matter) defined as follows

$$F_h+F_g+F_a+F_q=0, \tag{66}$$

where

$$F_h=-\frac{dP_r}{dr}, \tag{67}$$

$$F_g=-\frac{\nu'}{2}(\sigma+P_r), \tag{68}$$

$$F_a=\frac{2}{r}(P_t-P_r), \tag{69}$$

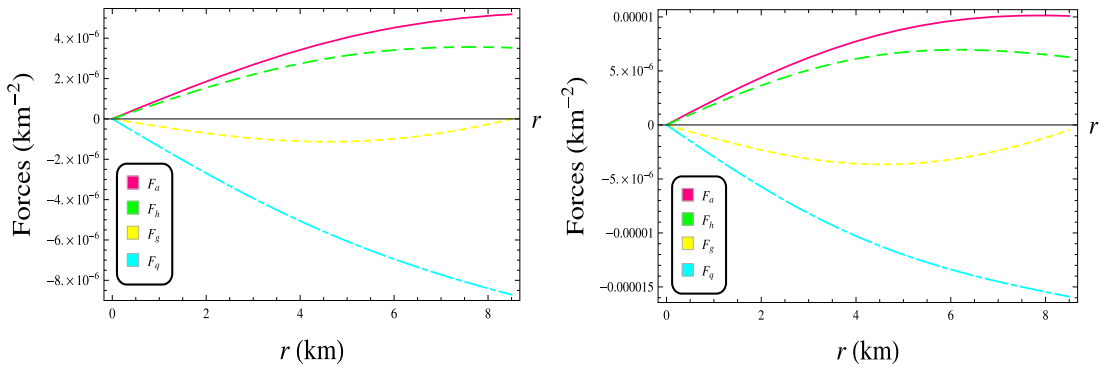

Figure 7. Variation of all forces for the stellar models Her X-1 (left panel) and SMC X-4 (right panel) versus r.

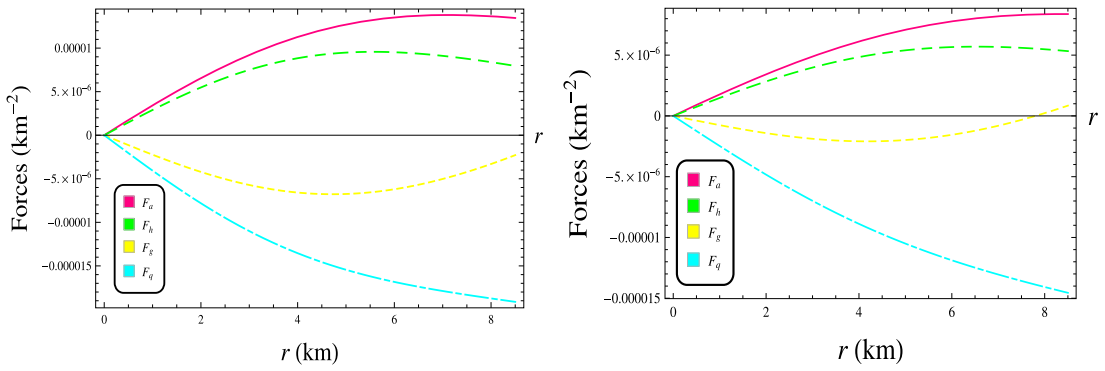

Figure 8. Variation of all forces for the compact stars Vela X1 (left panel) and 4U 1538-52 (right panel) versus r.

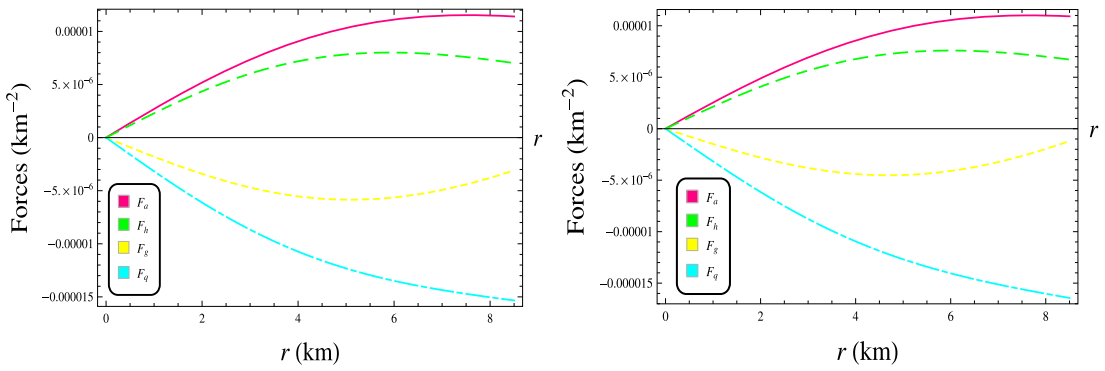

Figure 9. Variation of all forces for the compact stars PSR J1614-2230 (left panel) and Cen X-3 (right panel) versus r.

$$F_q = -\frac{\nu'}{2}(\sigma^q + P_r^q) - \frac{dP^q}{dr}. \tag{70}$$

The profiles of the F_h, F_g, F_a, and F_q forces for the model stars are displayed in figures 7–9. This figure shows that the proposed complexity-free hybrid star is in equilibrium under these forces.

5.4. Causality condition

An anisotropic relativistic fluid sphere that is physically viable must adhere to the causality condition, which requires that the radial and transverse sound speeds be less than unity. This specific constraint is referred to as the causality condition. The sound speeds associated with radial and transverse stress components are defined as

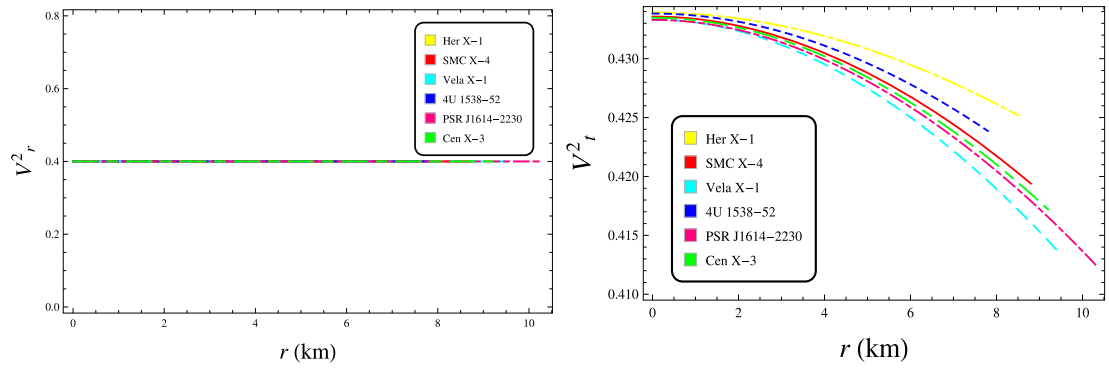

Figure 10. Plots of radial (V_r^2) (left panel) and transverse (V_t^2) (right panel) sound velocities versus r.

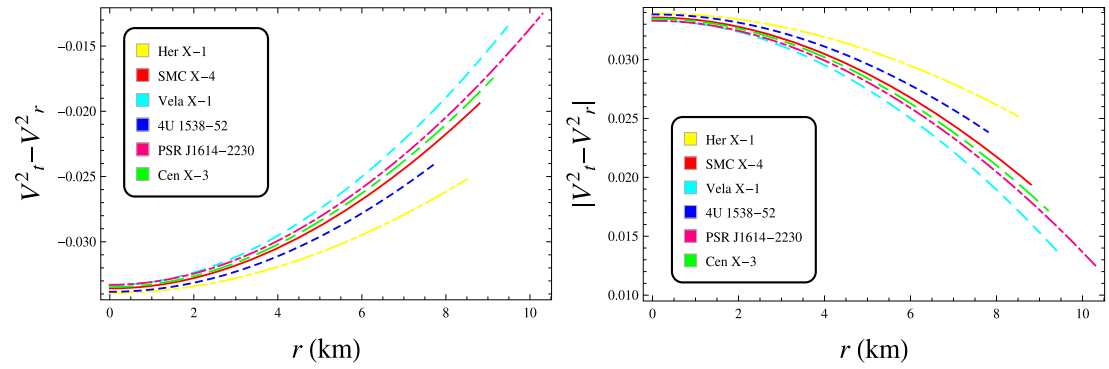

Figure 11. Plots of $V_t^2 - V_r^2$ (left panel) and $|V_t^2 - V_r^2|$ (right panel) versus r.

$$V_r^2 = \frac{dP_r}{d\sigma} = m, \tag{71}$$

$$V_t^2 = \frac{dP_t}{d\sigma}. \tag{72}$$

To verify the causality condition, we plot V_r^2 and V_t^2 versus r in figure 10 for the stellar models. We observe that both V_r^2 and V_t^2 satisfy the causality condition for the suggested solution. We now check if the proposed stellar model satisfies Herrera's cracking criterion [102]. The cracking scheme was employed by Abreu *et al* [103] to evaluate the stability bounds of astrophysical stellar distributions. Mathematically, a compact region is stable if $V_t^2 - V_r^2 < 0$. Figure 10 shows that throughout the complexity-free hybrid star, $0 < V_r^2 \leqslant 1$ and $0 < V_t^2 \leqslant 1$. Furthermore, our model also satisfies the condition $V_t^2 - V_r^2 < 0$, as demonstrated in the left panel of figure 11. Thus, we deduce that the proposed stellar solution is potentially stable. In addition, the conditions $0 < V_r^2 \leqslant 1$ and $0 < V_t^2 \leqslant 1$, along with $|V_t^2 - V_2^2| \leqslant 1$ [104], are satisfied, as described in the right panel of figure 11.

5.5. Relativistic mass and compactness

The compactness of the purposed stellar system is evaluated by the dimensionless parameter, which is the ratio of maximum mass to radius. This parameter has an upper limit. Buchdahl's limit [105] specifies that the compactness corresponding to the astrophysical compact configuration must be less than 4/9 in order to remain stable. To determine the compactness factor, we solve the following expression for the relativistic mass of compact structure, with the initial condition $m(0) = 0$.

$$\frac{dM^{eff}}{dr} = 4\pi r^2 \sigma^{eff}(r), \tag{73}$$

where $\sigma^{eff}(r) = \sigma(r) + \sigma^q(r)$. The integration of the above-mentioned differential equations with $m(0) = 0$ yields the mass of the complexity-free hybrid star as follows

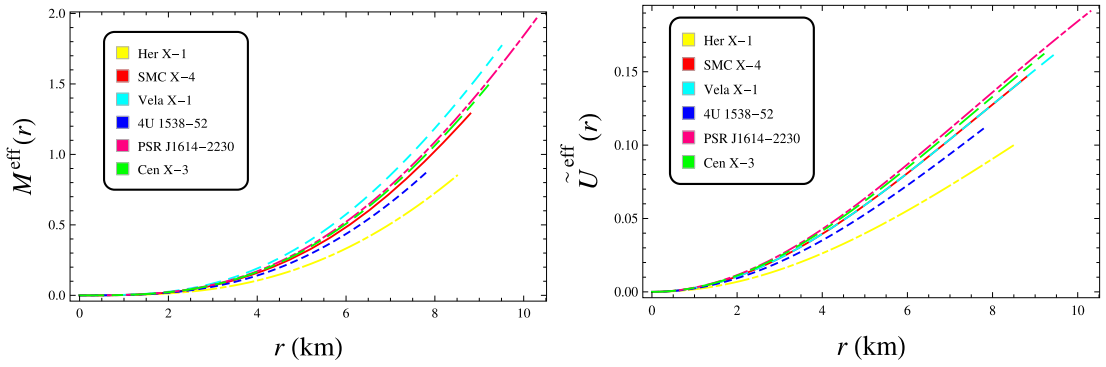

Figure 12. Plots of M^{eff} (left panel) and $\widetilde{U}^{eff}$ (right panel) versus r.

$$M^{eff}(r) = 4\pi \int_0^r r^2 \sigma^{eff}(r) = \frac{Sr^3}{2(1 + Sr^2)}. \tag{74}$$

According to equation (74), the effective mass M^{eff} vanishes at the central region, i.e., $M^{eff} \to 0$ as $r \to 0$, indicating the regularity of M^{eff} at the center. The variation of M^{eff} versus r is described in the left panel of figure 12. The mass M^{eff} is positive and increases monotonically with r within the complexity-free hybrid stellar distribution.

$$\widetilde{U}^{eff}(r) \equiv \frac{M^{eff}(r_\Sigma)}{r_\Sigma} = \frac{Sr^2}{2(1 + Sr^2)}. \tag{75}$$

The effective compactness behavior $\widetilde{U}^{eff}$ accosted with the complexity-free hybrid stellar system versus r is displayed in the right panel of figure 12. The plot of $\widetilde{U}^{eff}$ versus r shows a monotonically increasing trend and satisfies the upper bound 4/9.

5.6. Surface redshift

The surface redshift is one of the most significant variables in determining the compactness and gravitational strength of astrophysical formations. The intensity of the gravitational field surrounding a compact stellar configuration causes a shift in the frequency of light or radiation emitted from its surface. Higher redshift values indicate stronger gravity, which is often associated with stellar models such as NS and quark stars. It also acts as an observational tool to test theoretical models of stellar configurations, ensuring they are consistent with Einstein and other modified gravity models. The effective redshift function Z_s^{eff} the suggested complexity-free star is given by

$$1 + Z_s^{eff} \equiv (1 - 2\widetilde{U}^{eff})^{-\frac{1}{2}}. \tag{76}$$

Thus, the effective surface redshift Z_s^{eff} can be calculated as

$$Z_s^{eff} = \left(\frac{1}{1 + Sr^2}\right)^{-\frac{1}{2}} - 1. \tag{77}$$

According to Ivanov [106], the maximum value of Z_s for an anisotropic fluid sphere is 3.842 in the absence of Λ (the cosmological constant). As seen in figure 13, the redshift pattern associated with the complexity-free hybrid stellar system is consistent and well-behaved. The redshift curve starts at zero and then monotonically increases towards the surface.

5.7. Relativistic adiabatic index

This subsection aims to use the relativistic adiabatic index to ensure the stability of the suggested complexity-free hybrid star model. The equation governing the adiabatic index undergoes alterations when pressure anisotropy is present

$$\Gamma_r = \frac{\sigma + P_r}{P_r} V_r^2, \tag{78}$$

$$\Gamma_t = \frac{\sigma + P_t}{P_t} V_t^2, \tag{79}$$

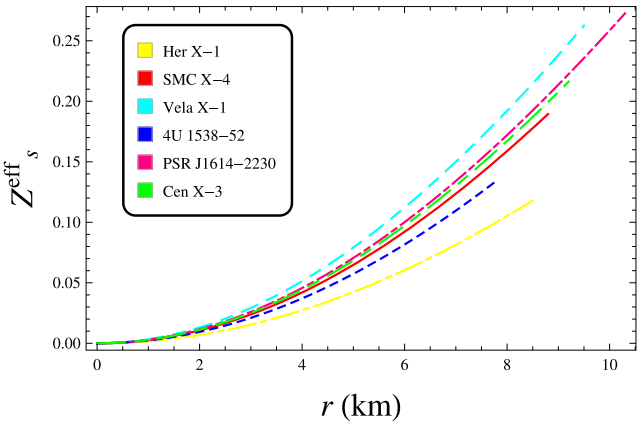

Figure 13. Plot of surface redshift versus r.

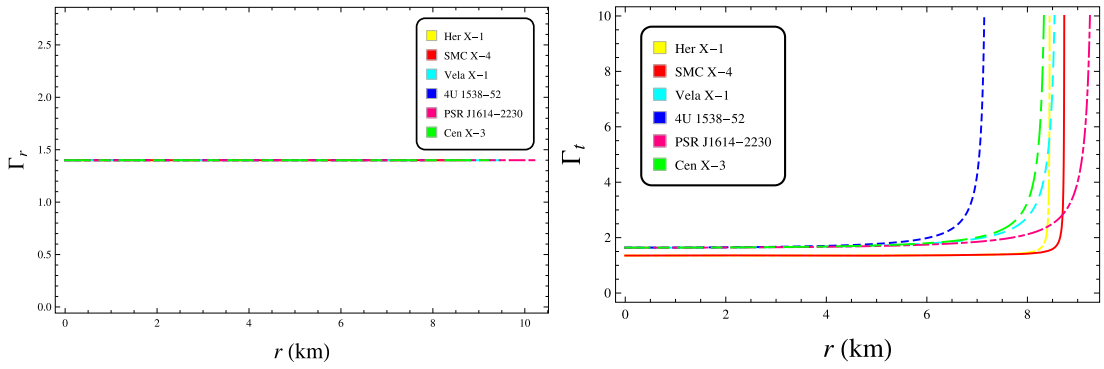

Figure 14. Plots of Γ_r and Γ_t versus r.

According to Heintzmann and Hillebrandt's analysis [107], the gravitationally bound system satisfies the conditions of stability when Γ_r and Γ_t take a value greater than 4/3. The equilibrium criterion requires that $\Gamma(r) > 4/3$ for $r < r_\Sigma$ within the gravitationally compact system, provided that $P_r \neq 0$ [107–110]. We have described the profiles of Γ_r and Γ_t for the considered model stars in figure 14. The graph demonstrates that both Γ_r and Γ_t maintain values greater than 4/3 throughout the complexity-free hybrid star, ensuring that the stability requirement is satisfied.

6. Conclusion

This paper investigates the construction of hybrid neutron stars with complexity-free characterization induced by orthogonal decomposition, using Einstein's gravitational model. In this model, we incorporate two separate fluid distributions: normal matter and quark matter. The strange matter is modeled using the EoS associated with the MIT bag model, $P_q = \frac{1}{3}(\sigma_q - 4B_g)$, while the baryonic matter is described by a linear EoS, $P_r = m\sigma$. Furthermore, we have incorporated the zero-complexity factor condition, which serves as an EoS to close the anisotropic gravitational configuration. This condition is employed to derive the temporal metric function; however, the radial metric function is considered based on the popular FK-ansatz, which is used as a seed metric for the proposed model.

Although some of the fundamental components of our research, such as the use of Einstein's gravitational equations and stress-energy tensors, are based on conventional methods, they provide a foundation for the exploration of new gravitational perspectives. In particular, our research offers the following novel insights:

1. This work incorporates the construction of a scalar function Y_{TF}, derived from the orthogonal decomposition of the Riemann curvature tensor. The quantity Y_{TF} characterizes the density inhomogeneity and pressure anisotropy, which are significant physical variables for exploring the underlying mechanisms of self-gravitational stellar configurations. This scalar quantity highlights the critical features of dense matter

configurations within a static and spherically symmetric framework. Several astrophysical investigations signify the role of Y_{TF} as an important structural element in the context of complex stellar systems [111, 112].

2. The analysis, emerging from the application of the vanishing complexity factor condition, is considered significant in determining several fundamental characteristics of the complex mechanisms involved in the development of compact, static, self-gravitational objects [62, 63].
3. The incorporation of the $Y_{TF} = 0$ condition plays a role in exploring the geometrical deformation of astrophysical dark systems with anisotropic matter content.
4. The coupling of the anisotropic stress-energy tensor with the MIT model, subject to the $Y_{TF} = 0$ constraint, gives rise to many hidden physical features inherent in gravitational dynamics and can be useful in describing the end states of compact configurations, including black holes, neutron stars, and other compact strange configurations [113–115].

We use the matching constraints between the interior geometry and the Schwarzschild outer geometry to determine the arbitrary constant parameters present in the anisotropic solution. We probe the physical consistency of our findings against six model stars: Her X-1, SMC X-4, Vela X-1, 4U 1538-52, PSR J1614-2230, and Cen X-3. The presented complexity-free hybrid neutron star model is well-behaved and free from central singularity. We analyze various astrophysical properties of hybrid stellar configurations, and the key findings related to the model are summarized as follows:

- The profiles of geometric variables is described in figure 1. Their profiles show that they meet the necessary conditions and are finite, positive, and free of singularities, i.e., $e^{\nu} = \left(B + \frac{A}{3S}\right)^2$ and $e^{\lambda} = 1$ as $r \to 0$. Both functions exhibit monotonic increasing behavior, attaining their maximum values at the boundary.
- The variations of stress components and matter density density against r are shown in figures 2 and 3. It is clear that σ, P_r, and P_t are non-negative and monotonically decreasing towards the boundary of the hybrid stellar distribution. Additionally, P_r vanishes at the boundary of each model star, which ensures the physical acceptability of the presented solution. The central values of σ, P_r, and P_t reveal that they exhibit their maximum at the core of compact configuration.
- The graph in figure 4 illustrates that the radial derivatives of P_r and σ are non-negative, ensuring that both quantities exhibit a decreasing trend as the radial distance r increases.
- Figure 3 (right panel) reveals an interesting gravitational effect by showing that $\Pi > 0$ for each model star, implying that the anisotropic force possesses a repulsive property. This positive value generates a repulsive force that keeps the star stable and prevents it from gravitational collapse.
- Figure 6 shows that the energy bounds corresponding to the complexity-free hybrid neutron star are satisfied for each model star.
- The equilibrium conditions for the hybrid stellar configuration have also been examined using the generalized equilibrium condition. Figures 7–9 illustrate the behavior of the forces F_a, F_h, F_g and F_q, showing that they are all stable and maintained equilibrium condition corresponding to each model star.
- The profiles of radial (V_r^2) and tangential (V_t^2) sound speeds for the proposed hybrid solution are described in figure 10. The dynamical equilibrium of the model is ensured by both V_r^2 and V_t^2 sound velocities being in accordance with Herrar's stability criterion as shown in figure 11.
- The positive values of the radial and tangential adiabatic index, i.e., $\Gamma_r = \Gamma_t > \frac{4}{3}$ describe the stable nature of the complexity-free hybrid neutron star as illustrated in figure 14.
- The variations of effective mass, compactness, and redshift are displayed in figures 12 and 13. All of these parameters are observed to exhibit a monotonic increase behavior with increasing r throughout the stellar distribution.

In this work, we established a new hybrid star framework where the matter content is described by two components: strange quark matter and regular matter. The model incorporates the well-known FS metric potential for the radial gravitational potential, along with a temporal gravitational potential derived from the complexity-free constraint. Although the interior composition and physical acceptability of such structures is the primary focus of our investigation, we acknowledge that observational parameters, such as R_{∞}, are crucial for bridging the gap between theoretical predictions and astrophysical observations. The proposed compact

configuration utilizes the MIT model for strange-quark matter and assesses its consistency with physical and observational constraints. The relativistic effects discussed in Haensel's work [116] are naturally incorporated into the model. Although the apparent radiation radius R_∞ is a crucial observable variable that could be addressed in future developments of our model, this work primarily assesses the coordinate radius R to characterize the star's structural features. The link between R and R_∞ is indirectly validated by the compactness and gravitational redshift analysis that are part of our work.

We have used a phenomenological approach to the phase transition from hadronic to quark matter. We do not enforce a sharp boundary or use a phase transition technique like Maxwell or Gibbs. On the contrary, we observe the star interior as a continuous mixing of hadronic and quark matter. This simplification enables us to obtain analytical results and leads to a continuous variation of thermodynamic quantities within the star. As a result, our model demonstrates the shift from hadronic to quark matter as a progressive process, yielding continuous profiles of pressure, energy density, and other thermodynamic parameters throughout the stellar interior. The contributions from both phases are effectively linked through the selected EoS and the metric structure, with no well-defined transition border. We recognize, however, that in more realistic scenarios, the nature of the phase transition depends on underlying microphysical assumptions.

- Employing a Maxwell construction results in a sharp, discontinuous phase transition of the first order, which is marked by a region of constant pressure and a sudden increase in density.
- The Gibbs construction allows for a continuous phase transition through a region where both phases coexist, with the transition parameters governed by surface tension and the effectiveness of charge screening.

We consider our present model a first approximation for investigating the overall behavior of hybrid stars, even though it does not explicitly distinguish between different phase transition methods.

In the future, it will be intriguing to explore whether the EoS for hybrid stars can account for neutron star cooling, magnetic fields, and anomalies in hybrid stellar structures. Additionally, this work can be extended to investigate charged strange stars by incorporating the effects of the electric field within Einstein's and higher-curvature gravitational models. To improve the relationship between theoretical radii and radiation observations, we plan to incorporate more explicitly R_∞ in subsequent research, building on Haensel's insights [116]. Direct comparisons between theoretical predictions and observed radiation parameters may be necessary to account for the impact of spacetime curvature on radiation transmission. Future analysis of branched quantum lattice and other physical applications [117–120] may be useful.

Declaration of competing interest

The authors have no conflict of interest regarding publication of the present paper.

CRediT authorship contribution statement

S.K., J.R.: Writing - review & editing, Supervision, Conceptualization, Writing - original draft, Visualization, Validation, Software, Methodology, Investigation. J.R., I.I., S.M., A.D.,A.A.: Validation, Methodology, Formal analysis. J.R., S.M., A.D., A.A.: Software, Methodology, Investigation. S. Khan:

Data availability statement

This manuscript contains no associated data. The data that support the findings of this study are available upon reasonable request from the authors.

References

[1] Lattimer J M and Prakash M 2000 Nuclear matter and its role in supernovae, neutron stars and compact object binary mergers *Phys. Rep.* **333** 121
[2] Oppenheimer J R and Snyder H 1939 On continued gravitational contraction *Phys. Rev.* **56** 455
[3] Tolman R C 1939 Static solutions of Einstein's field equations for spheres of fluid *Phys. Rev.* **55** 364
[4] Yousaf Z, Ganesan T, Almutairi B, Bhatti M Z and Khan S 2024 Effect of einasto spike on the gravitationally decoupled self-gravitating dark matter halos *Phys. Scr.* **99** 125302
[5] Yousaf Z, Bamba K, Almutairi B, Hashimoto Y and Khan S 2024 Imprints of dark matter on the structural properties of minimally deformed compact stars *Phys. Dark Universe* **46** 101629
[6] Albalahi A M, Yousaf Z, Khan S and Ali A 2024 Anisotropic interior models with Kohler-Chao-Tikekar-like complexity factor *Eur. Phys. J. C* **84** 963

[7] Yousaf Z, Bamba K, Almutairi B, Khan S and Bhatti M Z 2024 Role of complexity on the minimal deformation of black holes *Class. Quantum Grav.* **41** 175001
[8] Burns E 2020 Neutron star mergers and how to study them *Living Rev. Relativ.* **23** 4
[9] Glendenning N K 2012 *Compact stars: Nuclear physics, Particle Physics and General Relativity* (Springer Science & Business Media)
[10] Heiselberg H and Pandharipande V 2000 Recent progress in neutron star theory *Ann. Rev. Nucl. Part. Sci.* **50** 481
[11] Demorest P B, Pennucci T, Ransom S M, Roberts M S E and Hessels J W T 2010 A two-solar-mass neutron star measured using shapiro delay *Nature* **467** 1081
[12] Abbott B P *et al* 2017 GW170817: observation of gravitational waves from a binary neutron star inspiral *Phys. Rev. Lett.* **119** 161101
[13] Antoniadis J *et al* 2013 A massive pulsar in a compact relativistic binary *Science* **340** 1233232
[14] Fonseca E *et al* 2016 The nanograv nine-year data set: mass and geometric measurements of binary millisecond pulsars *Astrophys. J.* **832** 167
[15] Buballa M *et al* 2014 EMMI rapid reaction task force meeting on quark matter in compact stars *J. Phys. G* **41** 123001
[16] Abbott B P *et al* 2019 Properties of the binary neutron star merger GW170817 *Phys. Rev. X* **9** 011001
[17] Farhi E and Jaffe R L 1984 Strange matter *Phys. Rev.* D **30** 2379
[18] Itoh N 1970 Hydrostatic equilibrium of hypothetical quark stars *Progress Theor. Phys.* **44** 291
[19] Bodmer A R 1971 Collapsed nuclei *Phys. Rev.* D **4** 1601
[20] Alford M 2001 Color-superconducting quark matter *Ann. Rev. Nucl. Part. Sci.* **51** 131
[21] Pagliara G, Herzog M and Röpke F K 2013 Combustion of a neutron star into a strange quark star: The neutrino signal *Phys. Rev.* D **87** 103007
[22] Cheng K S, Dai Z G and Lu T 1998 Strange stars and related astrophysical phenomena *Int. J. Mod. Phys.* D **7** 139
[23] Glendenning N K 1992 First-order phase transitions with more than one conserved charge: consequences for neutron stars *Phys. Rev.* D **46** 1274
[24] Pagliara G and Schaffner-Bielich J 2008 Stability of color-flavor-locking cores in hybrid stars *Phys. Rev.* D **77** 063004
[25] Dexheimer V A and Schramm S 2010 Novel approach to modeling hybrid stars *Phys. Rev.* C **81** 045201
[26] Lenzi C H and Lugones G 2012 Hybrid stars in the light of the massive pulsar PSR J1614- 2230 *Astrophys. J.* **759** 57
[27] Orsaria M, Rodrigues H, Weber F and Contrera G A 2013 Quark-hybrid matter in the cores of massive neutron stars *Phys. Rev.* D **87** 023001
[28] Chen H, Wei J B, Baldo M, Burgio G and Schulze H J 2015 Hybrid neutron stars with the dyson-schwinger quark model and various quark-gluon vertices *Phys. Rev.* D **91** 105002
[29] Baldo M, Bombaci I and Burgio G F 1997 Microscopic nuclear equation of state with three-body forces and neutron star structure *Astron. Astrophys.* **328** 274
[30] Schulze H J, Polls A, Ramos A and Vidana I 2006 Maximum mass of neutron stars *Phys. Rev.* C **73** 058801
[31] Li Z H and Schulze H J 2008 Neutron star structure with modern nucleonic three-body forces *Phys. Rev.* C **78** 028801
[32] Ruderman M 1972 Pulsars: structure and dynamics *Ann. Rev. Astron. Astrophys* **10** 427
[33] Bowers R L and Liang E 1974 Anisotropic spheres in general relativity *Astrophys. J.* **188** 657
[34] Yousaf Z, Bhatti M Z and Khan S 2022 Stability analysis of isotropic spheres in einstein gauss-bonnet gravity *Ann. Phys.* **534** 2200252
[35] Sharif M and Yousaf Z 2015 Radiating cylindrical gravitational collapse with structure scalars in $f(R)$ gravity *Astrophys. Space Sci.* **357** 49
[36] Sharif M and Yousaf Z 2013 Electromagnetic field and dynamical instability of cylindrical collapse in $f(R)$ gravity *Mon. Not. R. Astron. Soc.* **432** 264–73
[37] Sharif M and Yousaf Z 2015 Instability of meridional axial system in $f(R)$ gravity *Eur. Phys. J. C* **75** 194
[38] Yousaf Z, Bhatti M and Farwa U 2017 Stability of compact stars in $\alpha R^2 + \beta(R^{\gamma\delta}T_{\gamma\delta})$ gravity *Mon. Not. R. Astron. Soc.* **464** 4509–19
[39] Bhatti M Z, Yousaf Z and Rehman A 2020 Gravastars in $f(R, G)$ gravity *Phys. Dark Universe* **29** 100561
[40] Yousaf Z 2025 Viscous fluid cosmology: A path to cosmic acceleration *Phys. Dark Universe* **48** 101884
[41] Aman H and Yousaf Z 2025 Neutron star analysis under $f(R, G, L_m)$ gravity model *J. High Energy Astrophys.* **47** 100380
[42] Herrera L and Santos N O 1997 Local anisotropy in self-gravitating systems *Phys. Rep.* **286** 53
[43] Battista E and De Falco V 2022 Gravitational waves at the first post-newtonian order with the weyssenhoff fluid in einstein-cartan theory *Eur. Phys. J. C* **82** 628
[44] Battista E and Steinacker H C 2022 On the propagation across the big bounce in an open quantum flrw cosmology *Eur. Phys. J. C* **82** 909
[45] Naseer T and Sharif M 2024 Charged anisotropic starobinsky models admitting vanishing complexity *Phys. Dark Universe* **46** 101595
[46] Naseer T and Sharif M 2024 Estimating the role of bag constant and modified theory on anisotropic stellar models *Chin. J. Phys.* **88** 10
[47] Battista E 2024 Quantum schwarzschild geometry in effective field theory models of gravity *Phys. Rev.* D **109** 026004
[48] Capozziello S, De Bianchi S and Battista E 2024 Avoiding singularities in lorentzian-euclidean black holes: The role of atemporality *Phys. Rev.* D **109** 104060
[49] Naseer T and Sharif M 2024 Decoupled anisotropic buchdahl's relativistic models in f ($\mathbb{R}$, $\mathbb{T}$) theory *Phys. Scr.* **99** 035001
[50] Naseer T 2024 Role of rastall gravity in constructing new spherically symmetric stellar solutions *Phys. Dark Universe* **46** 101663
[51] Naseer T 2024 Complexity and isotropization based extended models in the context of electromagnetic field: an implication of minimal gravitational decoupling *Eur. Phys. J. C* **84** 1256
[52] Yousaf Z 2025 Sustenance of isotropic pressure constraint in spherically symmetric object *Ind. J. Phys.* **99** 3149
[53] Calbet X and López-Ruiz R 2001 Tendency towards maximum complexity in a nonequilibrium isolated system *Phys. Rev.* E **63** 066116
[54] Catalán R G, Garay J and López-Ruiz R 2002 Features of the extension of a statistical measure of complexity to continuous systems *Phys. Rev.* E **66** 011102
[55] Sanudo J and Pacheco A 2009 Complexity and white-dwarf structure *Phys. Lett.* A **373** 807
[56] Sañudo J and López-Ruiz R 2008 Statistical complexity and fisher-shannon information in the h-atom *Phys. Lett.* A **372** 5283
[57] Chatzisavvas K C, Psonis V P, Panos C P and Moustakidis C C 2009 Complexity and neutron star structure *Phys. Lett.* A **373** 3901
[58] De Avellar M G B, De Souza R A, Horvath J E and Paret D M 2014 Information theoretical methods as discerning quantifiers of the equations of state of neutron stars *Phys. Lett. A* **378** 3481
[59] Herrera L 2018 New definition of complexity for self-gravitating fluid distributions: the spherically symmetric, static case *Phys. Rev.* D **97** 044010
[60] Herrera L, Di Prisco A and Ospino J 2018 Definition of complexity for dynamical spherically symmetric dissipative self-gravitating fluid distributions *Phys. Rev.* D **98** 104059

[61] Herrera L, Ospino J, Di Prisco A, Fuenmayor E and Troconis O 2009 Structure and evolution of self-gravitating objects and the orthogonal splitting of the Riemann tensor *Phys. Rev.* D **79** 064025
[62] Habsi M A, Maurya S, Badri S A, Al-Alawiya M, Mukhaini T A, Malki H A and Mustafa G 2023 Self-bound embedding class i anisotropic stars by gravitational decoupling within vanishing complexity factor formalism *Eur. Phys. J. C* **83** 286
[63] Panotopoulos G, Rincón Á. and Lopes I 2024 Anisotropic dark energy stars within vanishing complexity factor formalism: Hydrostatic equilibrium, radial oscillations, and observational implications *Phys. Lett.* B **856** 138901
[64] Contreras E and Fuenmayor E 2021 Gravitational cracking and complexity in the framework of gravitational decoupling *Phys. Rev.* D **103** 124065
[65] Das S, Sarkar N, Das A and Pal S K 2024 Anisotropic compact stellar model: a vanishing complexity approach *Eur. Phys. J. C* **84** 817
[66] Maieron C, Baldo M, Burgio G F and Schulze H J 2004 Hybrid stars with the color dielectric and the MIT bag models *Phys. Rev.* D **70** 043010
[67] Nicotra O E, Baldo M, Burgio G F and Schulze H J 2006 Hybrid protoneutron stars with the MIT bag model *Phys. Rev.* D **74** 123001
[68] Chen H, Baldo M, Burgio G F and Schulze H J 2011 Hybrid stars with the Dyson-Schwinger quark model *Phys. Rev.* D **84** 105023
[69] Bhar P 2015 A new hybrid star model in Krori-Barua spacetime *Astrophys. Space Sci.* **357** 46
[70] Bhar P, Pradhan S, Malik A and Sahoo P K 2023 Physical characteristics and maximum allowable mass of hybrid star in the context of $f(Q)$ gravity *Eur. Phys. J. C* **83** 646
[71] Alford M, Braby M, Paris M and Reddy S 2005 Hybrid stars that masquerade as neutron stars *Astrophys. J.* **629** 969
[72] Brilenkov M, Eingorn M, Jenkovszky L and Zhuk A 2013 Dark matter and dark energy from quark bag model *J. Cosmol. Astropart. Phys.* 002 **2013**
[73] Maharaj S, Sunzu J and Ray S 2014 Some simple models for quark stars *Eur. Phys. J. Plus* **129** 3
[74] Paulucci L and Horvath J E 2014 Strange quark matter fragmentation in astrophysical events *Phys. Lett.* B **733** 164
[75] Isayev A 2015 Stability of magnetized strange quark matter in the MIT bag model with a density dependent bag pressure *Phys. Rev.* C **91** 015208
[76] Lugones G and Arbañil J D 2017 Compact stars in the braneworld: a new branch of stellar configurations with arbitrarily large mass *Phys. Rev.* D **95** 064022
[77] Bhar P and Rahaman F 2015 The dark energy star and stability analysis *Eur. Phys. J. C* **75** 41
[78] Witten E 1984 Cosmic separation of phases *Phys. Rev.* D **30** 272
[79] Hackman R H, Deshpande N, Dicus D A and Teplitz V L M 1978 1 transitions in the MIT bag model *Phys. Rev. D* **18** 2537
[80] Haxton W and Heller L 1980 Heavy-quark-antiquark potential in the MIT bag model *Phys. Rev.* D **22** 1198
[81] Lopes L L, Biesdorf C and Menezes D P 2021 Modified mit bag models–part i: thermodynamic consistency, stability windows and symmetry group *Phys. Scr.* **96** 065303
[82] Klevansky S P 1992 The Nambu–Jona-Lasinio model of quantum chromodynamics *Rev. Mod. Phys.* **64** 649
[83] Herrera L, Di Prisco A and Ospino J 2020 Quasi-homologous evolution of self-gravitating systems with vanishing complexity factor *Eur. Phys. J. C* **80** 631
[84] Yousaf Z, Bhatti M Z, Khan S and Sahoo P K 2022 $f(\mathrm{G}, \mathrm{T}_{\alpha\beta}\mathrm{T}^{\alpha\beta})$ theory and complex cosmological structures *Phys. Dark Universe* **36** 101015
[85] Albalahi A M, Yousaf Z, Ali A and Khan S 2024 Isotropization and complexity shift of gravitationally decoupled charged anisotropic sources *Eur. Phys. J. C* **84** 9
[86] Khan S and Yousaf Z 2024 Complexity-free charged anisotropic Finch-Skea model satisfying Karmarkar condition *Phys. Scr.* **99** 055303
[87] Yousaf Z, Khan S, Turki N B and Suzuki T 2024 Modeling of self-gravitating compact configurations using radial metric deformation approach *Chinese J. Phys.* **89** 1595
[88] Casadio R, Contreras E, Ovalle J, Sotomayor A and Stuchlik Z 2019 Isotropization and change of complexity by gravitational decoupling *Eur. Phys. J. C* **79** 826
[89] Contreras E and Stuchlik Z 2022 A simple protocol to construct solutions with vanishing complexity by gravitational decoupling *Eur. Phys. J. C* **82** 706
[90] Finch M R and Skea J E F 1989 A realistic stellar model based on an ansatz of Duorah and ray *Class. Quantum Grav.* **6** 467
[91] Duorah H and Ray R 1987 An analytical stellar model *Class. Quantum Grav.* **4** 1691
[92] Delgaty M S R and Lake K 1998 Physical acceptability of isolated, static, spherically symmetric, perfect fluid solutions of Einstein's equations *Comput. Phys. Commun.* **115** 395
[93] Hansraj S, Chilambwe B and Maharaj S D 2015 Exact EGB models for spherical static perfect fluids *Eur. Phys. J. C* **75**
[94] Chanda A, Dey S and Paul B 2019 Anisotropic compact objects in $f(\mathrm{T})$ gravity with Finch-Skea geometry *Eur Phys. J. C* **79** 502
[95] Maurya S K 2019 A completely deformed anisotropic class one solution for charged compact star: a gravitational decoupling approach *Eur. Phys. J. C* **79** 958
[96] Maurya S K, Errehymy A, Jasim M K, Hansraj S, Al-Harbi N and Abdel-Aty A H 2022 A simple protocol for anisotropic generalization of Finch-Skea model by gravitational decoupling satisfying vanishing complexity factor condition *Eur. Phys. J. C* **82** 1173
[97] Gokhroo M K and Mehra A L 1994 *Gen. Relativ. Gravit.* **26** 75
[98] Abubekerov M K, Antokhina E A, Cherepashchuk A M and Shimanskii V V 2008 The mass of the compact object in the X-ray binary Her X-1/HZ her *Astron. Rep.* **52** 379
[99] Rawls M L, Orosz J A, McClintock J E, Torres M A P, Bailyn C D and Buxton M M 2011 Refined neutron star mass determinations for six eclipsing x-ray pulsar binaries *Astrophys. J.* **730** 25
[100] Barziv O, Kaper L, Van Kerkwijk M H, Telting J H and Van Paradijs J 2001 The mass of the neutron star in Vela X-1 *Astron. Astrophys.* **377** 925
[101] Baykal A L T A N, Inam S and Beklen E 2006 Recent timing studies on RXTE observations of 4U 1538-52 *Astron. Astrophys.* **453** 1037
[102] Herrera L 1992 *Phys. Lett.* A **165** 206
[103] Abreu H, Hernández H and Núnez L A 2007 Sound speeds, cracking and the stability of self-gravitating anisotropic compact objects *Class. Quantum Grav.* **24** 4631
[104] Andréasson H 2009 Sharp bounds on the critical stability radius for relativistic charged spheres *Commun. Math. Phys.* **288** 715
[105] Buchdahl H A 1959 General relativistic fluid spheres *Phys. Rev.* **116** 1027
[106] Ivanov B V 2002 Maximum bounds on the surface redshift of anisotropic stars *Phys. Rev.* D **65** 104011
[107] Heintzmann H and Hillebrandt W 1975 Neutron stars with an anisotropic equation of state-mass, redshift and stability *Astron. Astrophys.* **38** 51
[108] Bondi H 1964 The contraction of gravitating spheres *Proc. R. Soc. Lond. Ser. A. Math. Phys. Sci.* **281** 39

[109] Chan R, Herrera L and Santos N O 1993 Dynamical instability for radiating anisotropic collapse *Mon. Not. R. Astron. Soc.* **265** 533
[110] Moustakidis C C 2017 The stability of relativistic stars and the role of the adiabatic index *Gen. Relativ. Gravit.* **49** 68
[111] Arias C, Contreras E, Fuenmayor E and Ramos A 2022 Anisotropic star models in the context of vanishing complexity *Ann. Phys.* **436** 168671
[112] Maurya S K *et al* 2023 Role of vanishing complexity factor in generating spherically symmetric gravitationally decoupled solution for self-gravitating compact object *Eur. Phys. J. C* **83** 532
[113] Bogadi R S and Govender M 2022 Dynamical complexity and the gravitational collapse of compact stellar objects *Eur. Phys. J. C* **82** 475
[114] Oertel M, Hempel M, Klähn T and Typel S 2017 Equations of state for supernovae and compact stars *Rev. Mod. Phys.* **89** 015007
[115] Maurya S K *et al* 2024 Modeling compact object mergers GW190814 and GW200210 and other self-bound compact stars with dark matter induced by gravitational decoupling and its significance to the mass gap *Astrophys. J.* **972** 175
[116] Haensel P 2001 Apparent radii of neutron stars and equation of state of dense matter *Astron. Astrophys.* **380** 186
[117] Koussour M, Bekov S, Syzdykova A, Muminov S, Ibragimov I and Rayimbaev J 2025 Observational constraints on a generalized equation of state model *Phys. Dark Universe* **47** 101799
[118] Rakhmanov S, Matchonov K, Yusupov H, Nasriddinov K and Matrasulov D 2025 Optical high harmonic generation in dirac materials *Eur. Phys. J. B* **98** 35
[119] Akramov M, Eshchanov B, Usanov S, Norbekov S and Matrasulov D 2024 Second-harmonic generation in branched optical waveguides: metric graphs based approach *Phys. Lett.* A **524** 129827
[120] Akramov M, Trunk C, Yusupov J and Matrasulov D 2024 Discrete schrödinger equation on graphs: An effective model for branched quantum lattice *Europhys. Lett.* **147** 62001